REVIEW ARTICLE

WILEY

Mass spectrometry analysis of saponins

Philippe Savarino | **Marie Demeyer** | **Corentin Decroo** | **Emmanuel Colson** |
Pascal Gerbaux

Organic Synthesis and Mass Spectrometry Laboratory, Biosciences Research Institute, University of Mons—UMONS, Mons, Belgium

Correspondence
Pascal Gerbaux, Organic Synthesis and Mass Spectrometry Laboratory, Biosciences Research Institute, University of Mons—UMONS, 23 Place du Parc, B-7000 Mons, Belgium.
Email: pascal.gerbaux@umons.ac.be

Abstract

Saponins are amphiphilic molecules of pharmaceutical interest and most of their biological activities (i.e., cytotoxic, hemolytic, fungicide, etc.) are associated to their membranolytic properties. These molecules are secondary metabolites present in numerous plants and in some marine animals, such as sea cucumbers and starfishes. Structurally, all saponins correspond to the combination of a hydrophilic glycan, consisting of sugar chain(s), linked to a hydrophobic triterpenoidic or steroidic aglycone, named the sapogenin. Saponins present a high structural diversity and their structural characterization remains extremely challenging. Ideally, saponin structures are best established using nuclear magnetic resonance experiments conducted on isolated molecules. However, the extreme structural diversity of saponins makes them challenging from a structural analysis point of view since, most of the time, saponin extracts consist in a huge number of congeners presenting only subtle structural differences. In the present review, we wish to offer an overview of the literature related to the development of mass spectrometry for the study of saponins. This review will demonstrate that most of the past and current mass spectrometry methods, including electron, electrospray and matrix-assisted laser desorption/ionization ionizations, gas/liquid chromatography coupled to (tandem) mass spectrometry, collision-induced dissociation including MS^3 experiments, multiple reaction monitoring based quantification, ion mobility experiments, and so forth, have been used for saponin investigations with great success on enriched extracts but also directly on tissues using imaging methods.

KEYWORDS
glycan, imaging, ion mobility, natural product, saponin

1 | INTRODUCTION

Saponins form an important class of natural products first discovered in plants (Kofler & Adam, 1927) and then in a few marine organisms such as sea stars (asteroids) (Yasumoto et al., 1966), sea cucumbers (holothuroids) (Yasumoto et al., 1966), and sponges (Stonik, 1986). Saponins are widespread plant specialized metabolites (Osbourn et al., 2003). In a systematic study done on 1730 Asian plant species, 76% were shown to contain saponins and many plants and vegetables consumed in the human diet contain saponins (Kassem et al., 2014).

The term "saponin" comes from the Latin word "sapo" meaning soap, whereas the suffix "ine" has been added as the signature of a chemical substance. Saponins are indeed present in different plants, such as soaproot (*Chlorogalum pomeridianum*) and soapberry (*Sapindus saponaria*), whose extracts have been employed as soap for years (Oleszek & Hamed, 2010). These biomolecules are glycosides that arise from the condensation of one or more oligosaccharide chains, called glycan, onto an aglycone moiety of steroidal or triterpenoid nature. A typical saponin structure is presented in Figure 1 and corresponds to scabraside A (**1**) found in *Holothuria scabra*, a sea cucumber from Madagascar (Caulier, Flammang, Rakotorisoa, et al., 2013). Both elements are mainly connected via a glycosidic linkage; even though some saponins present an ester bond associating the glycan and the aglycone parts. Other chemical functionalities can be appended on the saponin core-structure, such as a carboxylate function ($-COO^-$) (Yoshikawa et al., 1996), a sulphate group ($-SO_4^-$) (Demeyer et al., 2014) or different acylated functions (Kanchanapoom et al., 2001). A huge amount of different saponin molecules has already been characterized, but it is suspected that more congeners are still to be detected.

These molecules are thus characterized by a large chemical diversity and a wide variety of biological activities (Desai et al., 2009), making them of high interest for the pharmaceutical companies due to their hemolytic, cytotoxic, antibacterial, antifungal, antiviral, and antitumor properties

(Desai et al., 2009). Paradoxically, their biological roles in the host organisms are still very speculative. Different studies have reported that animal saponins are also involved in several activities such as chemical defense (Mackie et al., 1975) and interspecific chemical communication (Caulier, Flammang, Gerbaux, et al., 2013). The role of saponins in plant is primarily associated to the defense against invading harmful organisms (fungi, bacteria) and predators (insects) (Arabski et al., 2012; Chaieb, 2017; Mert-Türk & Osbourn, 2006).

The extreme structural diversity of saponins makes them challenging from a structural analysis point of view since, most of the time, saponin extracts consist in a huge number of congeners presenting only subtle structural differences (Wei et al., 2005). Saponin analysis by mass spectrometry methods is nowadays progressively supplementing other analytical methods such as nuclear magnetic resonance (NMR). Indeed, saponin extracts from plant or marine animals are often constituted by a complex mixture of (slightly) different saponin molecules that requires extensive purification and separation steps to meet the requirement for NMR spectroscopy measurements. Based on its intrinsic features, mass spectrometry represents an inescapable tool to access the structures of saponins within extracts by using liquid chromatography mass spectrometry (LC-MS), matrix-assisted laser desorption/ionization mass spectrometry (MALDI-MS), electron ionization, high resolution mass spectrometry (HRMS), tandem mass spectrometry and ion mobility experiments. In this review, we will not provide a
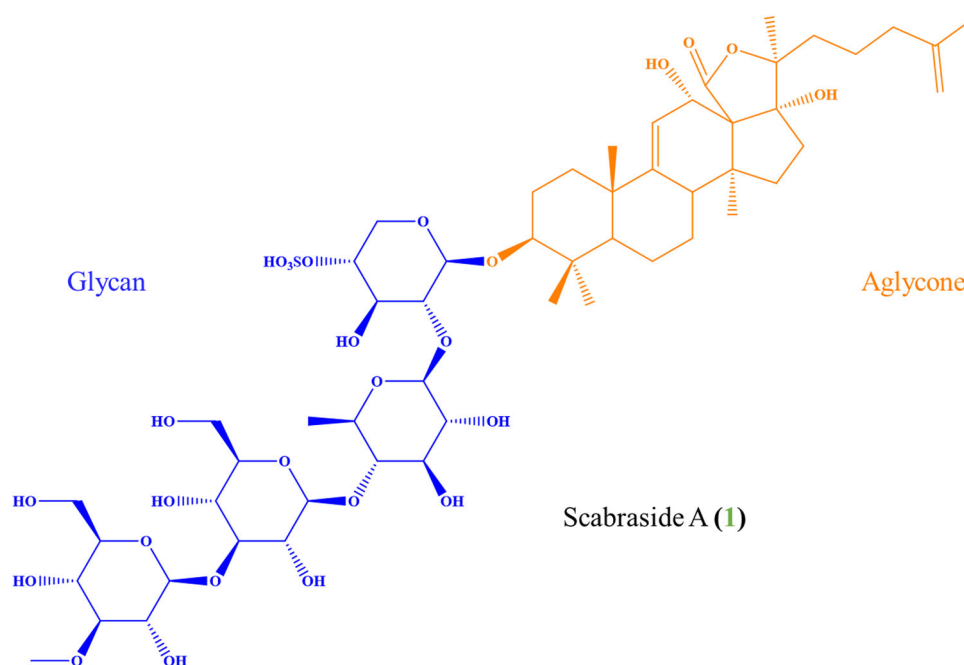
FIGURE 1 Structure of Scabraside A (1), a saponin found in *Holothuria scabra*, composed of a glycan (left) and an aglycone (right) (Caulier, Flammang, Rakotorisoa, et al., 2013) [Color figure can be viewed at wileyonlinelibrary.com]

complete review of the literature describing the use of mass spectrometry for the characterization of saponins. This would be totally unnecessary, if not impossible. Indeed, a quick search on Scopus (March 03, 2021) using as keyword "saponin AND mass spectrometry" generates no less than 3812 references. We rather intend to combine references presenting the different techniques of mass spectrometry which have been used for the study of saponins. In doing so we will certainly omit to cite important works of eminent colleagues and we already apologize for it.

2 | SAPONIN MOLECULAR STRUCTURES

### 2.1 | The apolar part of saponin: The aglycone

The molecules belonging to the crowded saponin family are first classified according to their aglycone structure. Three classes of (sapo)genins, i.e. triterpenoid, steroid and steroid alkaloid, have been to date identified and are presented in Figure 2. Triterpenoid aglycones contain 30 carbon atoms, whereas steroid aglycones count 27 carbon atoms, as

respectively exemplified by β-amyrin (2) and cholestanol (3) in Figure 2. Note also that a numeration of the carbon atoms specific to the sapogenins has been established by Maier and is also presented in Figure 2 (Maier, 2008).

The main sapogenins retrieved in plants are the triterpenoids β-amyrin (2), α-amyrin (4), and lupeol (5); whereas the steroids furostane (6) and spirostane (7) are only scarcely detected (Haralampidis et al., 2002; Yang et al., 2014). Steroid alkaloids, amongst which spirosolane (8) and solanidane (9) in Figure 2 are typical examples, constitute a class of genins presenting a nitrogen atom in the backbone (Ghisalberti, 2006). Specificity in the aglycone structure is also characteristic of the animal saponins. For instance, holostanol (10) and lanosterol (11) are specific to sea cucumbers and cholestanol (3) is detected in some sea star species (Maier, 2008).

2.2 | The polar part of saponin: The glycan

The monosaccharide residues constituting the glycan part of saponins are extremely diversified and largely contribute to the saponin diversity and structure complexity.
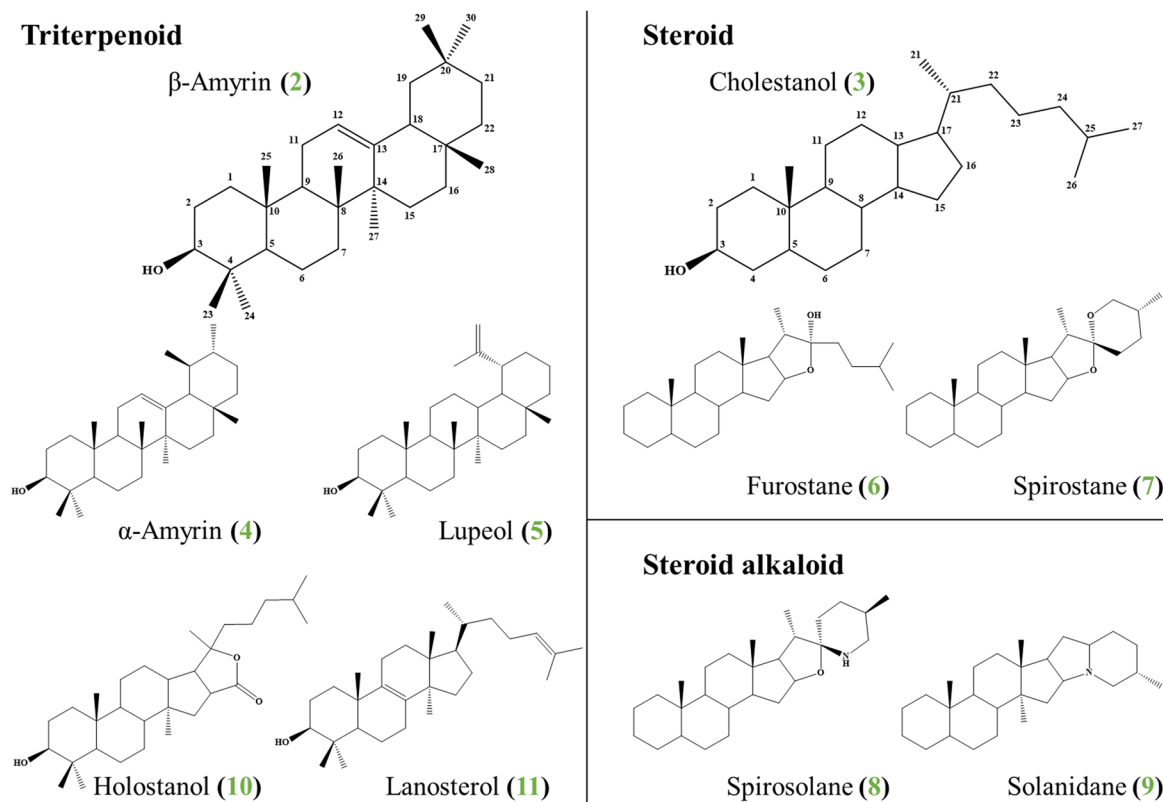
FIGURE 2 The aglycone diversity composed of three main classes: triterpenoid, steroid and steroid alkaloid with the Maier numeration for β-amyrin (2) and cholestanol (3) (Ghisalberti, 2006; Haralampidis et al., 2002; Maier, 2008; Yang et al., 2014) [Color figure can be viewed at wileyonlinelibrary.com]

In plants, β-D-glucose (Glc), β-D-glucuronic acid (GluA), β-D-rhamnose (Rha), and β-D-arabinose (Ara) and their epimeric forms, that is, β-D-galactose (Gal) or β-D-xylose (Xyl), are abundantly encountered (Vincken et al., 2007; Augustin et al., 2011). In marine invertebrates, the glycan part includes other monosaccharides such as 3-O-methylglucose (3-OMe-Glc) in sea cucumbers (Caulier, Flammang, Rakotorisoa, et al., 2013) or 6-deoxy-xylo-hex-4-ulose in sea stars (Demeyer et al., 2014). The oligo-saccharidic chains mostly count from one to six sugar residues, even if some glycans composed of 10 units have already been reported in *Clematoside mandshurica* (Khorlin et al., 1965). Additionally, the oligosaccharide chain can be linear or branched (Sahu et al., 2008).

Finally, saponins can be subdivided in different families according to their glycan topology. *Monodesmosidic* saponins are characterized by the condensation of a single oligosaccharide onto the aglycone, whereas *polydesmosidic* structures appear when several oligosaccharide chains are linked onto the aglycone. Typical examples are presented in Figure 3 and correspond to desholothurin A (Khorlin), present in *Holothuria forskali* (Rodriguez, Castro, & Riguera, 1991), and saponin B (13) found in *Chenopodium quinoa* Willd. seeds (Kuljanabhagavad et al., 2008)

Besides these two families, macrocyclic topologies are also known and correspond to molecules with a single oligosaccharide chain attached at two sites on the agly-cone. A typical example is presented in Figure 3 and correspond to sepositoside A (14) detected in the saponin extracts from the sea star *Echinaster sepositus* (De Simone et al., 1981).

2.3 | One step further toward the structural complexity: Specific chemical functions

Saponins are glycosidic molecules associating two distinct parts and characterized by an extreme structural diversity that is further exacerbated by the presence of substituents presenting specific chemical functions. As a typical example, saponins in several marine animals present one or several sulfate groups on either the agly-cone or the glycan parts depending on the animals (Demeyer et al., 2014; Kang et al., 2015). In sea stars, this sulfate group is specifically localized on the aglycone (Demeyer et al., 2014), while it is present on the first xylose residue of the oligosaccharide chain in several sea
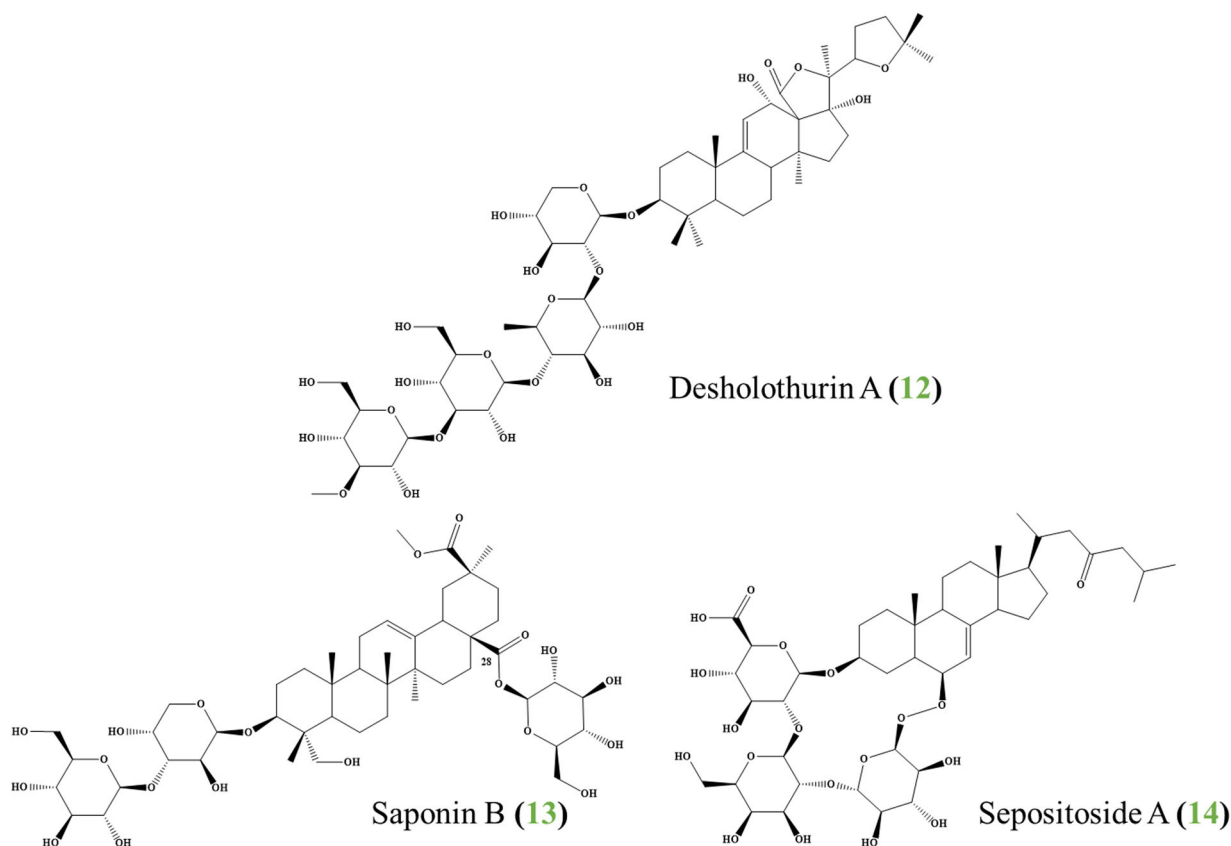
FIGURE 3 Different saponin topologies including monodesmosidic (**12**), bidesmosidic (**13**), and macrocyclic (**14**) structures (Kuljanabhagavad et al., 2008; Rodriguez et al., 1991; De Simone et al., 1981) [Color figure can be viewed at wileyonlinelibrary.com]

cucumbers (Caulier, Flammang, Rakotorisoa, et al., 2013). In *Aesculus hippocastanum* seeds, the escin (**15**) molecules compose a family of saponins that are structurally related but present some minute differences such as the structure of the side chains (Figure 4) on the sapogenin (Yoshikawa et al., 1996). A symptomatic example is related to the aglycone substitution at C21, where five different acyl groups have been detected: tiglic acid (Tig), angelic acid (Ang), acetic acid (Ac), isobutyric acid (A), and 2-methylbutyric acid (B) (Yoshikawa et al., 1996). Moreover, a second acetyl function can be localized in C22 or C28 (Yoshikawa et al., 1996).

3 | SAPONIN EXTRACTION FROM THE BIOMASS

For isolation of saponins, the majority of the numerous protocols present in the literature are based on successive liquid-liquid extractions with solvents of increasing polarity (Campagnuolo et al., 2001; Garneau et al., 1983). As for a typical example, our extraction method has been adapted from the literature and consists in different liquid/liquid extractions (Van Dyck et al., 2009). The weighed biomass powder is stirred in methanol for 24 h at room temperature followed by centrifugation. The supernatant is diluted to 70% methanol with Milli-Q water. This hydromethanolic extracts is partitioned (v/v) successively against *n*-hexane, chloroform and dichloromethane to remove impurities such as fatty acids. Finally, the hydromethanolic solution, containing saponins, is evaporated at low pressure. The dry extract is solubilized in Milli-Q water to undergo a last partitioning against isobutanol

(v/v). The butanolic phase is washed twice with Milli-Q water to remove residual salts and impurities. The organic solution containing the saponins is evaporated to dryness. The dry residue obtained after evaporation is weighed and stored in the fridge at 4°C.

Solid phase extraction (SPE) protocols are also optimized for biological sample cleanup and saponin preconcentration before the MS analysis. Numerous studies report the use of C18 SPE phases for the pretreatment of saponins, including triterpenoidal saponins contained in rat plasma that are quite complex and present at very low concentrations (Wang et al., 2007; Xu et al., 2011). Microwave-assisted extraction has been demonstrated to show outstanding saponin extraction efficiency compared to other conventional extraction methods, such as ultrasonic extraction and heat reflux extraction, on *Pulsatilla turczaninovii* (Xu et al., 2012).

4 | BOTTOM-UP APPROACHES FOR SAPONIN IDENTIFICATION

Saponin structural characterization may be performed using a bottom-up strategy meaning that the saponin molecules are first decomposed upon hydrolysis into their building blocks that are further analyzed using online gas chromatography (GC-MS) or liquid chromatography (LC-MS) mass spectrometry experiments.

Upon acid conditions (aqueous HCl), all the glycosidic linkages, being acetal functions, are hydrolyzed producing the sapogenin residues together with all the free monosaccharides. These building blocks are further analyzed upon GC-MS after derivatization. Trimethylsilyl ether derivatives are usually preferred since (i) they are formed within a few
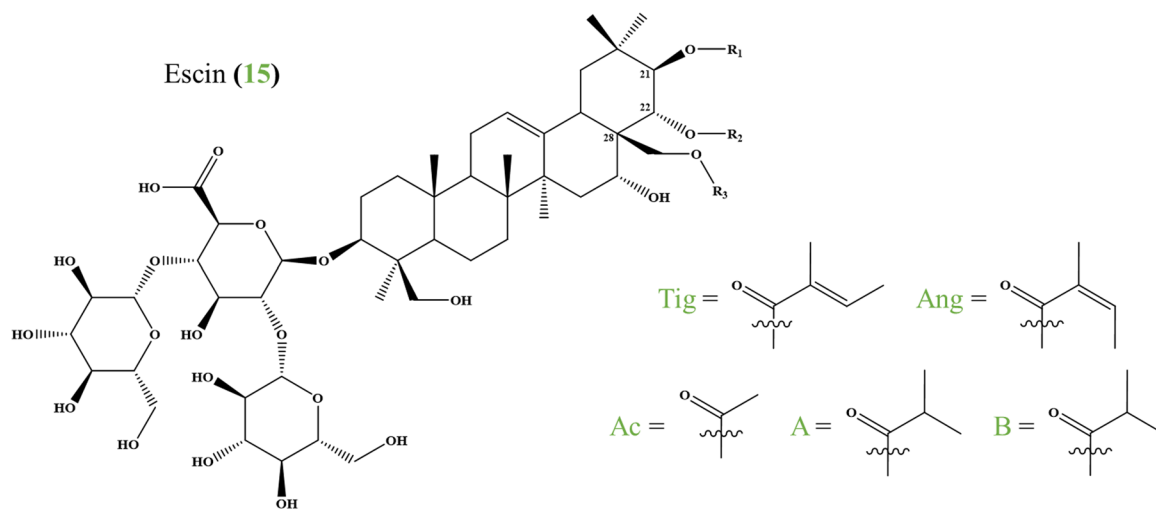

FIGURE 4 Molecular structures of Escin (**15**) molecules extracted from *Aesculus hippocastanum* seeds where Tig, Ang, Ac, A, and B correspond to tiglic acid, angelic acid, acetic acid, isobutyric acid and 2-methylbutyric acid, respectively. Adapted from (Yoshikawa et al., 1996) [Color figure can be viewed at wileyonlinelibrary.com]

minutes at room temperature using reagents such as *N,O*-bis-(trimethylsilyl)trifluoroacetamide (Burnouf-Radosevich et al., 1985) or trimethylsilyl cyanide (Jæger et al., 2017) and (ii) silylation avoids peak tailing and shortens considerably the retention time of triterpenes as compared to methylation and acetylation (Ikekawa et al., 1965). As a typical example, the acid hydrolysis of ligulataside A (**16**) (Figure 5), extracted from the Australian medicinal and food plant *Acacia ligulate*, results in the aglycone echinocystic acid (**17**) (red structure, Figure 5), and free saccharide units (Jæger et al., 2017) that are further identified upon GC-MS analysis. Identification of the aglycone moieties is often achieved on the basis of accurate mass measurements and comparison with commercially available standards. The analysis of the fragment ions generated upon electron ionization (EI-MS) mass spectra of triterpenes and related compounds is also nicely documented in older literature (Budzikiewicz et al., 1963). In general, the presence of an endocyclic double bond controls the fragmentation behavior, and characteristic mass spectral features have been noted which frequently allow assignment of a given triterpene in one of the major classes by this criterion. In addition, the location of functional groups can often be narrowed down by consideration of the fragmentation pattern (Budzikiewicz et al. 1963).

Alkaline hydrolysis is more specific than its acidic counterpart in the sense that glycosidic linkages are not hydrolyzed under basic conditions. This is particularly interesting in the case of bidesmosidic saponins, such as ligulataside A (**16**), when the second saccharide chain is appended onto the aglycone via an ester bond, see Figure 5. Alkaline hydrolysis of **16** produces a prosaponin (**18**) (red and pink structure, Figure 5), which can be analyzed by LC-MS/MS (Jæger et al., 2017). In a recent, study, we took advantage of the fast and homogeneous

microwave heating to specifically hydrolyze under basic conditions the bidesmosidic saponins extracted from *C. quinoa* into their monodesmosidic counterparts (Colson et al., 2020). The microwave-assisted hydrolysis reaction was optimized to quantitatively produce monodesmosidic saponins. The membranolytic activity of the saponins (ability of saponins to interact with the membrane leading to its lysis) was assayed based on their hemolytic activity that was shown to be drastically increased upon hydrolysis (Colson et al., 2020).

Enzymatic hydrolysis and structural determination by LC-MS/MS is another elegant procedure for the identification of saponins. Enzymes obtained from various plants and animals have been used for hydrolyzing polysaccharides, which resulted in the release of free sugar units depending on their specific activities according to the glycosidic bond positions (Jeong et al., 2014). Enzymatic transformation of natural molecules, such as platycosides (**19**), was introduced to modify the structures of natural molecules to reach enhanced pharmacological activities (Jeong et al., 2014). Enzymatic transformation by hydrolases was further implemented to selectively hydrolyze glycosidic linkages in platycosides (**19**) to discriminate isomers (Jeong et al., 2014). Platycosides (**19**) are saponins extracted from Platycodi Radix and are used as traditional medicines (Nyakudya et al., 2014). There are bidesmosidic saponins with an oligosaccharide moiety of arabinose, rhamnose, and xylose in sequence being attached onto the pentacyclic triterpenoid aglycone through an ester linkage at C-28 and the other being constituted by two or three β-glucose residues linked through linear glycosidic bonds at the C-3 position. Isomers of platycosides (**19**) are classified by the linkage positions of glycan linked at the C-3 position of the triterpene aglycone and are constitutional isomers

Ligulatadise A (**16**)
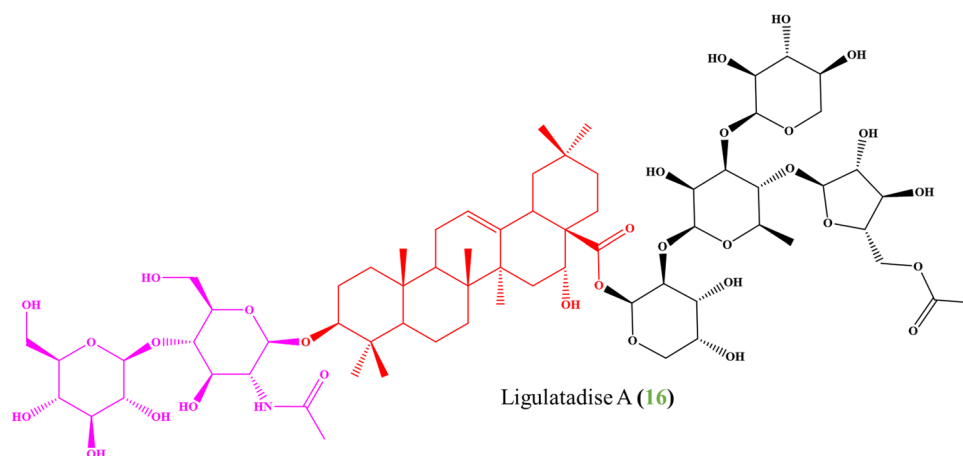
FIGURE 5 Molecular structure of ligulataside A (**16**) extracted from *Acacia ligulate* (Jæger et al., 2017) [Color figure can be viewed at wileyonlinelibrary.com]

with Glc-(1→6)-Glc or Glc-(1→3)-Glc glycosidic linkages (Nyakudya et al., 2014). Discrimination between those isomers may be achieved by selective glycosidic linkage hydrolysis using selected enzymes. For instance, glucosidases have a specific activity toward the Glc-(1→4)-Glc glucan, whereas glucanases predominantly hydrolyze Glc-(1→3)-Glc linkages and laminarinases show sufficient selectivity for hydrolyzing Glc-(1→6)-Glc linkages. After hydrolyzing a saponin extract by laminarinases, the reconstructed total ion chromatogram generated by a chemometric technique sorted peaks of deglycosylated platycosides easily discriminating the platycoside constitutional isomers without any LC-MS/MS experiments (Jeong et al., 2014).

Another approach combining hydrolysis, derivatization and GC-MS analysis has been recently introduced for saponin analysis and is inspired by the procedure developed by Pettolino et al. for determining the polysaccharide composition of plant cell walls based of the preparation of partially permethylated alditol acetates (PMMAs) (**20**) (Pettolino et al., 2012). The method starts by the permethylation of the saponin molecules using methyl iodide and sodium hydroxide in dimethyl sulfoxide. Complete methylation results in the methylation of all free hydroxyl groups not involved in the glycosidic linkage. After acid hydrolysis using trifluoracetic acid, the partially methylated monosaccharides that are released are reduced with sodium borodeuteride ($NaBD_4$) to simultaneously open the sugar ring to form alditol derivatives and tag the anomeric C atom (C1) with a deuterium atom. To further increase the volatility of the derivatives for GC separation, the partially methylated alditols are acetylated with acetic anhydride derivatives to produce PMMAs that are further analyzed using GC-MS (Jæger et al., 2017). Based on the MS fragmentation pattern of PMMAs ions and comparison with standard molecules, the monosaccharide present in the sample, together with their glycosidic linkage positions, are identified (Jæger et al., 2017).

5 | TOP-DOWN APPROACHES FOR SAPONIN IDENTIFICATION

The chemical or enzymatical hydrolysis of saponins has been previously demonstrated to afford valuable pieces of information for saponin analysis. However, as stated by Costello in her seminal publication related to the tandem mass spectrometry analysis of saponins: "Structural determinations of saponins present challenges to the analyst because of the variety of potential modification sites, the incorporation of both carbohydrate and non-carbohydrate moieties, and the occurrence of mixtures that may include isomeric species and highly-active

minor components" (Costello, 1996). Hence, hydrolysis eliminates the possibility to confirm the structure of intact saponins since, by definition, only building bricks are identified. This is even more inextricable that the hydrolyses are often carried out on mixtures of saponins.

The introduction of fast atom bombardment (FAB) mass spectrometry in 1981 has provided a rapid method for determining the molecular weights of involatile glycosides (Adinolfi et al., 1984), such as saponins. In 1984, Adinolfi et al. used muscaroside A (**21**) and digitonin (**22**) as model compounds to demonstrate the capabilities of FAB mass spectrometry for the structural analysis of saponins (Adinolfi et al., 1984). They showed that the molecular weights of intact saponin molecules can be readily determined using exact mass measurements on the protonated $[M + H]^+$ and sodium cationized $[M + Na]^+$ molecules. Further, they also detected in-source fragmentation reactions that were shown to occur at every glycosidic bond by a proton rearrangement from the leaving group to the interglycosidic oxygen (Adinolfi et al., 1984). They concluded that FAB fragment ions can be used to define the glycoside sequence but remains inefficient to differentiate isomeric hexoses or to identify the type of linkage between sugar residues. However, this study definitively paved the way to the soon coming reports on the tandem mass spectrometry analysis of saponin ions.

5.1 | Tandem mass spectrometry analysis of saponin ions

Tandem mass spectrometry, that is, collision-induced dissociation (CID) experiments, is now largely acknowledged as a powerful structural analysis method for saponins. Considerable structural information, indicating the nature of the aglycone and the linkage and position of the monosaccharide residues, may be deduced from the analysis of the CID spectra of $[M + H]^+$, $[M-H]^-$ and $[M + Cat]^+$ (Cat = Li or Na) ions. As a general rule, the fragmentation reactions undergone by activated saponin ions almost occur within the glycan part of the saponin ions, although dissociation reactions specific to the aglycone part may be sometime detected. Basically, upon CID of saponin ions, the sequence and the branching of the glycan moiety as well as the molecular mass of the intact aglycone can be obtained when the CID experiments are conducted under both low (collision energy (CE) < 100 eV) and high (CE > keV) collision energy conditions (Zehl et al., 2007). However, it is important to note that the distinction between isomeric aglycones is scarcely achieved using CID experiments (Zehl et al., 2007).

In 1988, Domon and Costello introduced their systematic nomenclature for carbohydrate fragmentations
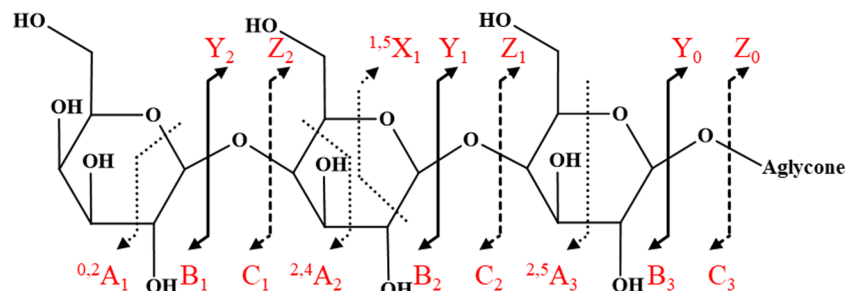
FIGURE 6 Carbohydrate fragmentation pathways where A_i, B_i, and C_i designate fragment ions containing the nonreducing end sugar unit, X_j, Y_j, and Z_j represent ions still containing the aglycone or the reducing end sugar unit. Subscripts indicate the position of the dissociated glycosidic bond relative to the reducing end, whereas superscripts indicate dissociations within carbohydrate rings. Adapted from (Domon & Costello, 1988) [Color figure can be viewed at wileyonlinelibrary.com]

in (FAB) MS/MS spectra of glycoconjugates (Domon & Costello, 1988). They also summarized all the fragment ions generated upon CID of ionized glycoconjugates (glycosphingolipids, glycopeptides, glycosides, and carbohydrates) in both the positive and negative ion modes.

As shown in Figure 6, the simplest fragmentation of the carbohydrate chain in collision activated saponin ions results from the cleavage of the glycosidic bond, that is, Y/B and Z/C pathways, yielding information regarding the sugar sequences. More complex processes involving the fragmentation within the sugar ring leading to the A fragment ions, are observed. Interestingly, both positive and negative ions present these fragmentation routes. As shown in Figure 6, A_i, B_i and C_i labels designate fragment ions containing the nonreducing end sugar unit, whereas X_j, Y_j and Z_j represent ions still containing the aglycone or the reducing end sugar unit. Subscripts indicate the position of the dissociated glycosidic bond relative to the reducing end (the glycosidic bond at the aglycone side is numbered 0), whereas superscripts indicate cleavages within carbohydrate rings (Domon & Costello, 1988). Specific nomenclature has also been introduced for branched saccharide chains.

Low-energy and high-energy CID spectra of $[M + H]^+$ saponin ions have been compared by Claeys et al. (1996) using a hybrid EBQQ and a four-sector EBEBE instruments, respectively. They demonstrated that low-energy CID fragmentations of sugar residues generate abundant Y_n^+ ions and some low intensity Z_n^+ ions, whereas the high-energy spectra also exhibit strong $^{1,5}X_n^+$ fragment ions, formed by multiple cleavage of the sugar ring, and significant Z_n^+ ions (Claeys et al., 1996). Zehl et al. performed a tandem mass spectrometry study on triterpenoid saponins isolated from *Bacopa monnieri*. They reported the application of different MS methods by associating data generated on ESI-ion trap (IT), atmospheric pressure MALDI-ion trap (AP-MALDI-IT) and MALDI-IT/reflectron time-of-flight (MALDI-IT-RToF)

for the low-energy CID and MALDI-ToF/RToF for the high-energy CID analysis (Zehl et al., 2007) on $[M + H]^+$ and $[M + Cat]^+$ (Cat = Na and K) precursor ions. The principal outcome of this large investigation is that, upon CID, whatever the nature of the precursor ions, low-energy and high-energy CID yield abundant B, C, Y, and Z fragment ions together with internal cleavage ions, with a global coverture of the glycosidic bonds. They also confirmed that abundant $^{1,5}X$ fragment ions are generated upon high-energy conditions (Zehl et al., 2007).

From a mechanistic point of view, the glycosidic bond dissociation generating B_i and Y_j ions (see Figure 7), with retention of the glycosidic oxygen atom by the species formed from the reducing end, is most of the time detected from $[M + H]^+$, $[M + Cat]^+$ and $[M-H]^-$ precursor ions (Domon & Costello, 1988). In the positive ion mode, it is proposed that the decomposition reaction of $[M + H]^+$ ions involves the protonation of the oxygen atom of the glycosidic bond which is broken affording the B_i oxonium ion (see Figure 7). Before the transient ion/neutral complex decomposition, a proton transfer may occur leading to the production of the complementary Y_j ions (Figure 7).

Negative ion decomposition mechanisms were also studied and were proposed to follow a more complex pathway, involving deprotonation of a hydroxyl group in position 3 (or 4), epoxidation, sugar ring opening and glycosidic bond rupture to yield Y_j fragment ions as shown in Figure 8 (Prome et al., 1987). Interestingly, from $[M-H]^-$ precursor ions, the dissociation of the glycosidic bond with retention of the glycosidic oxygen atom on the nonreducing end side is frequently observed and afford C and Z-type ions.

In that case, after deprotonation of a hydroxyl group adjacent to the glycosidic bond, the resulting alkoxy may undergo an epoxidation with rupture of the glycosidic bond, generating C-type ions, see Figure 8. Again, Z-type ions can be competitively produced upon proton transfer before the dissociation of the transient ion/neutral complex (Prome et al., 1987).
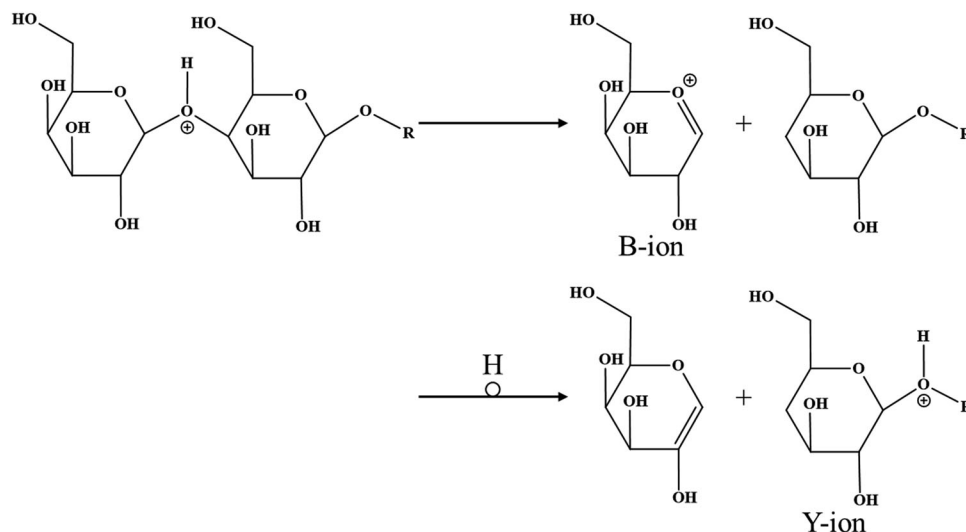
FIGURE 7 Production of B_i and Y_j fragment ions in the positive ion mode induced by protonation at the oxygen atom of the glycosidic bond. Adapted from (Domon & Costello, 1988)

Asterosaponins (23) are sulfated saponins with the sulfate group being attached on the aglycone moiety, see Figure 9. Consequently, since the negative charge is localized on the sulfate group, all the CID processes are shown to afford fragment ions containing the aglycone moiety or part of the aglycone moiety, that is to say Y-type ions (see Figure 6) and the CID reactions (low-energy conditions) were shown to formally correspond to the unwinding of the oligosaccharide chains converging to the aglycone part. However, no mechanistic study has been performed to date to decipher the position and role of the negative charge in the dissociating ions.

Fragmentations involving the aglycone side-chain may also be observed and, for instance, the asterosaponin 1 (24) ions in Figure 9 were observed, under low-energy conditions, to expel 100 u that arises from a McLafferty side-chain loss reaction, specific to the asterosaponin 1 (24) aglycone (Demeyer et al., 2014). Gevrenova et al. reported a large LC-MS/MS study related to the profiling of the saponins extracted from the roots of *Gypsophila trichoma* Wend (Gevrenova et al., 2018). These saponins are glucuronide oleanane-type triterpenoid carboxylic acid 3,28-O-bidesmosides (GOTCAB) (25) (see Figure 10). These saponins presenting a glucuronic acid at the C3 position are abundantly detected as [M-H]⁻ ions in the negative ion mode. Interestingly, some congeners present a sulphate group on a sugar residue on the C28 chain, making a huge difference with the asterosaponin 1 (24) previously described. Fragmentation pathways for the identification of those saponins were proposed in that study. Sulphated saponin ions were shown to expel 80 u, corresponding to a SO_3 neutral loss, as a primary dissociation from the [M-H]⁻ ions

(Gevrenova et al., 2018). For other saponin ions extracted from the same source, a 42 u loss, that is, neutral ketene, detected in the MS/MS spectra revealed the presence of an acetyl group. A competitive loss of 204 u further confirmed that those saponins contain an acetylated glucose moiety (Gevrenova et al., 2018).

Saikosaponins (27) (Figure 11) are monodesmosidic saponins and are considered to be the major bioactive ingredients of *Bupleurum chinense*, also known as Radix Bupleuri, which is a famous traditional Chinese medicine (Liu et al., 2019). Liu et al. detected six malonylated saikosaponins and two acetylated ones in the methanolic extract of *B. chinense* using LC-MS experiments. They developed a MS/MS-based protocol to discriminate between the aglycone-substituted and the saccharide-substituted saponins. They showed that, the $Y_0 - nH_2O$ (n = 1–2) fragment ions containing or not the substituent are observed in the CID mass spectra of the [M + H]⁺ ions of aglycone-substituted or saccharide-substituted saikosaponins, respectively. Interestingly, the B ions containing or not the substituent are rather observed from the [M + Na]⁺ ions of, respectively, the saccharide-substituted or aglycone-substituted saikosaponins (Liu et al., 2019). These results also clearly point to the fact that the CID reactions undergone by the [M + H]⁺ and [M + Na]⁺ saponin ions may be different due to the structural differences for the [M + H]⁺ versus [M + Na]⁺ precursor ions.

CID mass spectra of the [M + Li]⁺ saponin ions were recorded for standard dioscins (28) (Song et al., 2004) and ginsenosides (29) from *Panax ginseng* (Song et al., 2005) and CID experiments were demonstrated to be really efficient to allow isomeric saponin ion discrimination
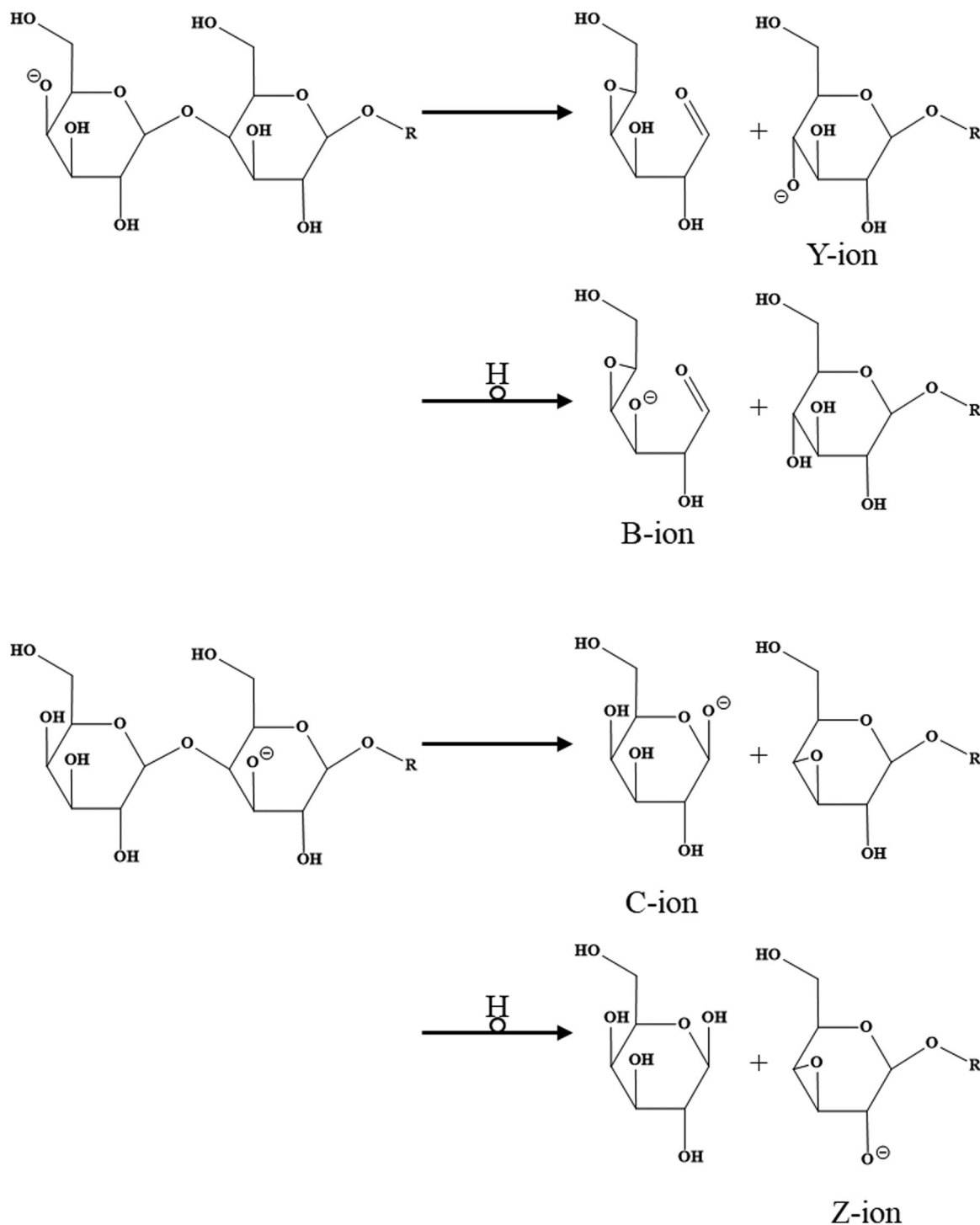
FIGURE 8 Production of B_i/Y_j ions and C_i/Z_j ions in the negative ion mode. Adapted from (Adinolfi et al., 1984; Domon & Costello, 1988)

since cross-ring cleavage product ions, i.e. X, A, Y and C type fragment ions, are observed to be abundant. CID experiments conducted on $[M-H]^-$ and $[M + Li]^+$ ions are often combined to get accurate structural information on the way to saponin structure identification (Lin et al., 2007; Song et al., 2005).

## 5.2 | Saponin characterization: Selected examples

Nowadays, FAB-MS and liquid secondary ion mass spectrometry (Costello, 1996) experiments are advantageously replaced by Electrospray ionization (ESI) and Matrix-assisted
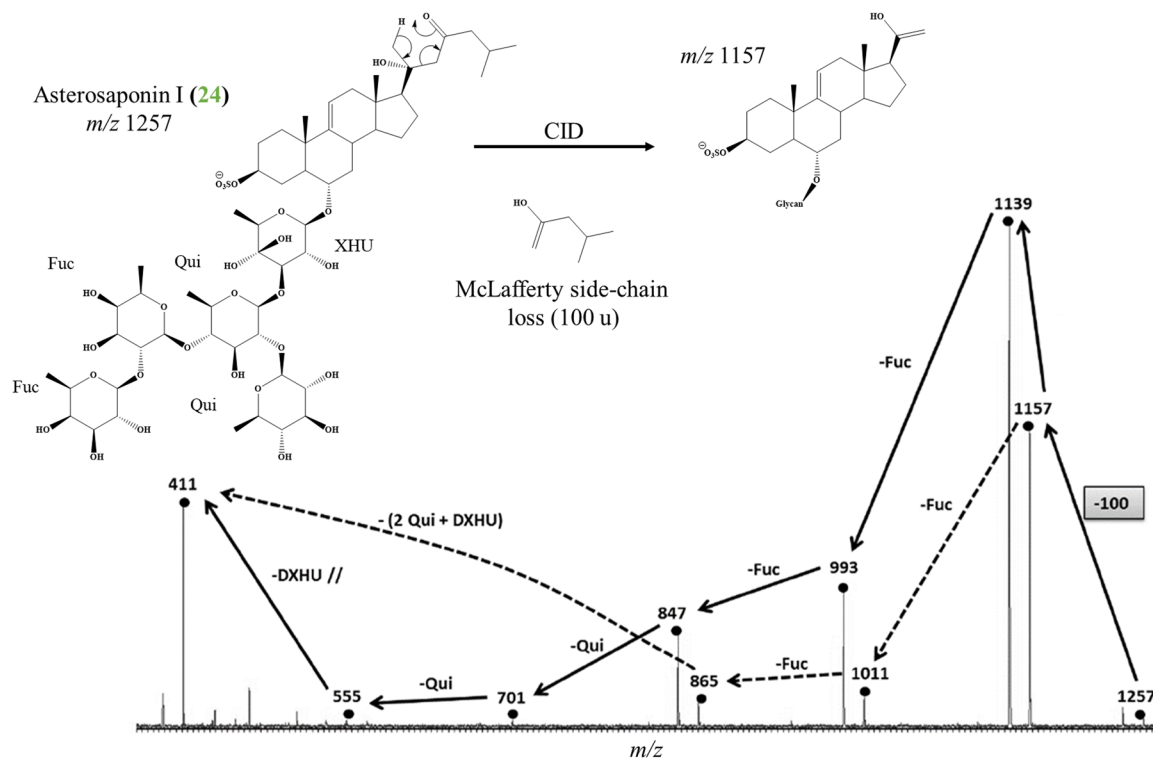
FIGURE 9 LC-MS/MS analysis (negative ion mode) of *m/z* 1257 ions. The CID activation leads to the loss of 100 u, characteristic of a McLafferty rearrangement specific to the presence of the aglycone side-chain of asterosaponin 1 (**24**). Adapted from (Demeyer et al., 2014) [Color figure can be viewed at wileyonlinelibrary.com]
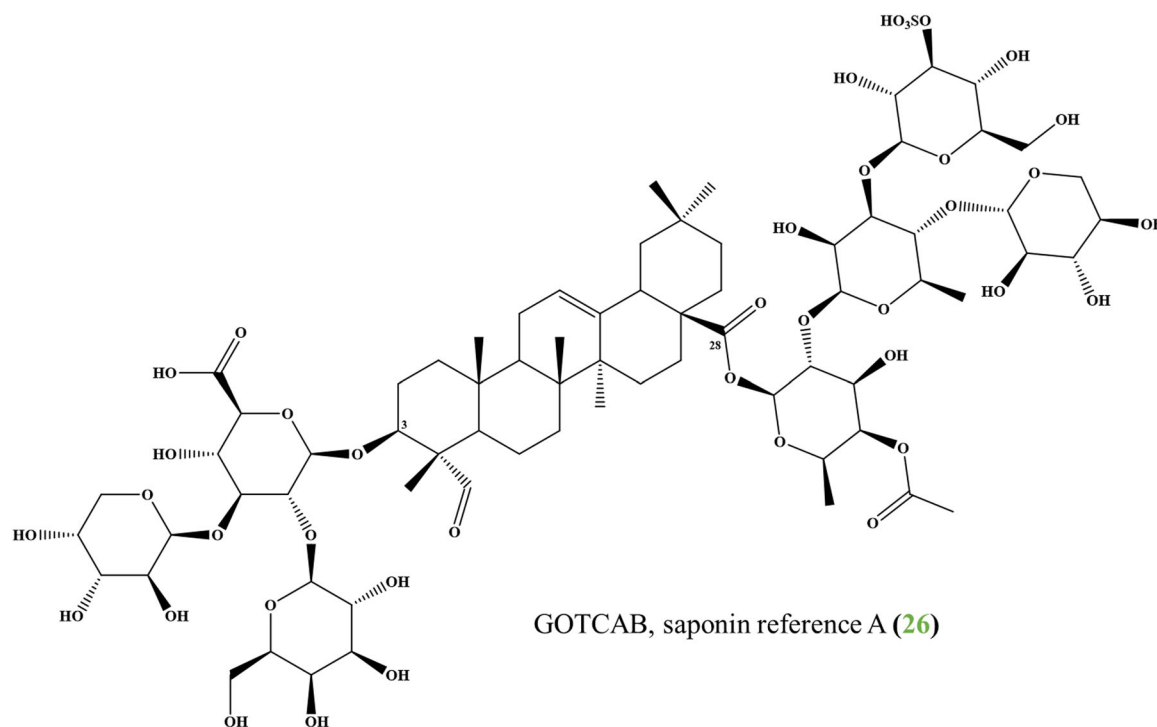
FIGURE 10 Saponin reference A (**26**), a glucuronide oleanane-type triterpenoid carboxylic acid 3,28-O-bidesmoside extracted from the roots of *Gypsophila trichoma* Wend (Gevrenova et al., 2018) [Color figure can be viewed at wileyonlinelibrary.com]
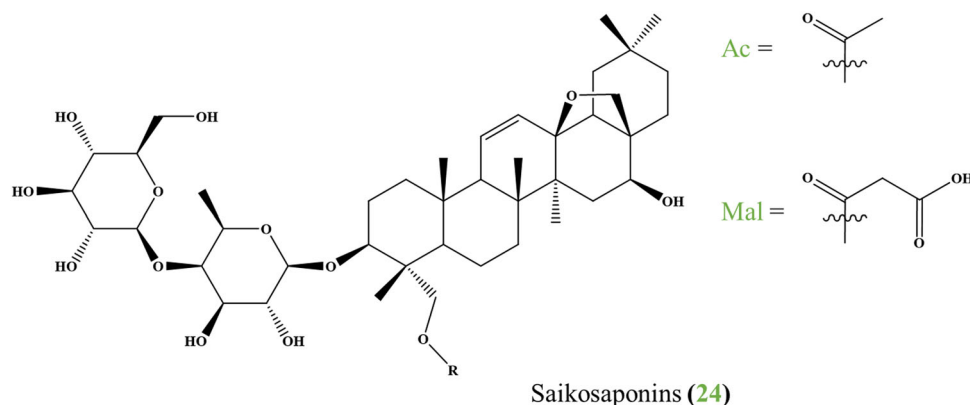
FIGURE 11 Saikosaponins (27) extracted from *Bupleurum chinense* where R can correspond to acetic acid (Ac) or malonic acid (Mal). Adapted from (Liu et al., 2019) [Color figure can be viewed at wileyonlinelibrary.com]

Laser desorption/ionization (MALDI) for the efficient and soft detection of intact saponin ions (Demeyer et al., 2014). CID experiments are also nowadays conducted on all the standard mass spectrometers, namely Q3 (Chen et al., 2019), Q-ToF (Zheng et al., 2017), FT-ICR (Zhang et al., 2010), ion trap (Wang et al., 2015), Orbitrap (Gevrenova et al., 2019), and QTrap (Shi et al., 2020).

Although unable to discriminate between isomeric saponins, MALDI-MS is often used for a rapid screening of the saponin content in an extract and for exact mass measurements when associated to a high resolution analyzer, such as orthogonal acceleration time-of-flight (oa-ToF) (Bahrami & Franco, 2015; Demeyer et al., 2014) and Fourier transform ion cyclotron resonance (FT-ICR) instruments (Bondoc et al., 2013). For instance, Bondoc et al. investigated the saponin contents of semi-purified and high-performance liquid chromatography (HPLC) fractionated extracts from the body wall of three species of Holothuriidae to examine their chemical diversities in relation to phylogenetic data. MALDI-FTICR-MS and nano-HPLC-chip Q-ToF-MS were used for mass profiling and isomer separation, respectively, giving a unique chemical saponin fingerprint (Bondoc et al., 2013). Obviously, the combination between reversed phase liquid chromatography (RP-LC) and ESI-MS is much more effective for the analysis of saponins enabling the possibility of separating the isomers before MS and MS/MS analysis (Kite et al., 2004; Li et al., 2012; Lin et al., 2007; Sandvoss et al., 2000, 2001, 2003)). As for a typical example from our lab, we used LC-MS and LC-MS/MS to highlight the molecular diversity and the body distribution of saponins in the sea star *Asterias rubens* (Demeyer et al., 2014). Asterosaponins (23) are well-known secondary metabolites of the common sea star *A. rubens* in which they would be involved in chemical defense, digestion, and reproduction. In this study, we analyzed separately the saponin content of different organs using the combination between MALDI-MS

and LC-MS/MS analyses. MALDI-MS experiments allowed for a rapid screening of the saponin mixtures, while LC–MS techniques were used to achieve chromatographic separation of isomers. In addition to the seventeen molecules (twelve compositions) already described in the literature (Sandvoss et al., 2000, 2001, 2003), we detected nine new molecules (six compositions). The comparison of the saponin contents from the five different body components revealed that each organ is characterized by a specific mixture of saponins and that qualitative and quantitative variability of the saponin contents are also linked to the sex or to the collecting season (Demeyer et al., 2014). From a biological point of view, this type of data is of crucial importance in understanding the biological role of these specific metabolites. Similarly, Popov et al. (2017) applied LC-MS/MS on the whole body extract and extracts of various body components to get a full description of the saponins present in the sea cucumber *Eupentacta fraudalix* that is living in the shallow waters of the south Part of the Sea of Japan. They identified 54 compounds, including 26 sulfated, 18 nonsulfated and 10 disulfated triterpene glycosides. By comparing the saponin contents of the different extracts, they demonstrated that the profiles of the different body components are qualitatively similar and that only small quantitative variabilities are observed (Popov et al., 2017).

Bahrami et al. also used the efficient combination between MALDI-MS/MS and LC-MS/MS for identifying the saponins present in the viscera of *Holothuria lessoni*, an Australian sea cucumber. The saponins were obtained by successive liquid/liquid extractions and further purified by high performance centrifugal partition chromatography. They detected 75 saponins, including 39 new congeners with a high structural diversity; revealing that the viscera samples possess a higher diversity and content than the body wall (Bahrami, Zhang, Franco, et al., 2014). In a second investigation, they used MALDI-MS and LC-MS/MS

to elucidate the structure of five novel isomeric saponins (Bahrami, Zhang, Chataway, et al., 2014).

Quillaja saponaria saponins possess extremely complexed structures that consist of the triterpene quillaic acid aglycone substituted at C3 with a di- or trisaccharide and at C28 with a complex oligosaccharide (Nord & Kenne, 1999). The first monosaccharidic residue of the latter glycan is an acyl-substituted fucosyl residue, linked via an ester bond at C28 of the aglycone (see Figure 12). As for an example, *Quillaja* saponin B1 (**30**) is presented in Figure 12 and is characterized by a complexed fattyl acyl residue on the fucosyl residue. The CID spectrum—MS^2—of the $[M + Na]^+$ ions is totally dominated by two signals, annotated $[A + Na]^+$ and $[B + Na]^+$ in Figure 12. The corresponding fragment ions arise from the cleavage of the glycosidic bonds linking the C3 and C28 oligosaccharides to the triterpene, respectively. The dissociation of the glycosidic bond at C3 affords $[A + Na]^+$ Y ions, whereas the rupture of the glycosidic bond at C28 yields $[B + Na]^+$ ions consisting of only the C28 oligosaccharide (including a formed insaturation in the fucose residue), see Figure 12. In other words, such a MS^2 mass spectrum does not contain any information regarding the detailed structures of the oligosaccharide chains at both

C3 and C28. Bankefors et al. (2011) therefore developed a multistep MS^3 strategy on an ion-trap instrument to recover the information about the structures of the C3 and C28 glycan groups, including regioisomer distinction

Beside structural characterization, CID experiments may also be of great interest for reaching higher sensitivity and selectivity for saponin detection on wide dynamic ranges by using multiple reaction monitoring (MRM) experiments. As for a striking example, Chen et al. (2016) developed an MRM-based strategy for the detection of ginsenosides (**29**) extracted from *Panax notoginseng*, the so-called Notoginseng total saponin (NGTS) extract, using a Sciex Q-trap 4500 mass spectrometer. $[M + HCOO]^-$ anions are usually detected as the dominant ions for gingenosides (**29**) under LC-MS(-) conditions using formic acid as the mobile phase addictive. By monitoring the formate anion-to-deprotonated ion transitions, that is, $[M + HCOO]^- \rightarrow [M-H]^-$ reaction, they detected 112 saponins, including 107 trace components and 12 potential new gingenosides (**29**).

A mass spectrometry-based database for rapid identification of saponins has been recently developed by Huang et al. (2020) and is referred to as saponin mass spectrometry database. The freely available database
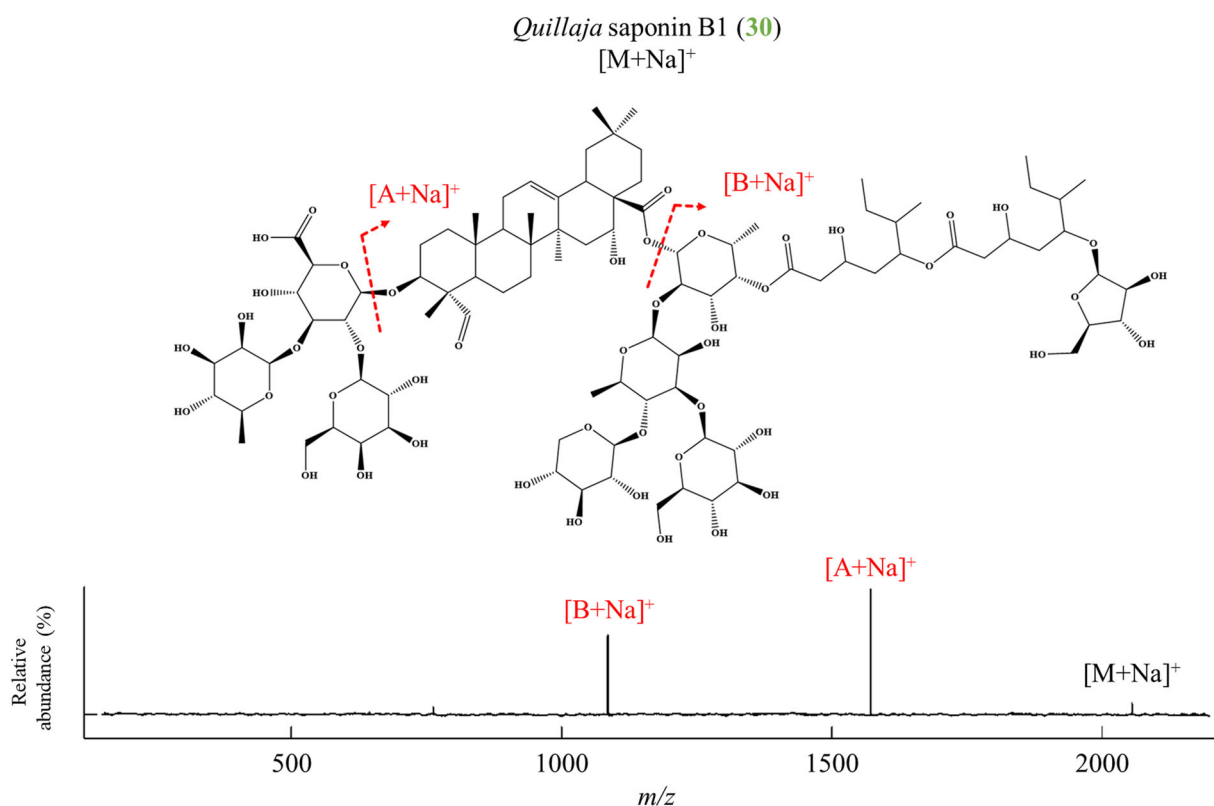
FIGURE 12 ESI-IT-MS/MS analysis (positive ion mode) of *m/z* 2055 ions, *Quillaja* saponin B1 (30) $[M + Na]^+$. The CID activation leads to the production of two major signals annotated $[A + Na]^+$ and $[B + Na]^+$, respectively arising from the cleavage of the glycosidic bonds linking the C3 and C28 oligosaccharides to the triterpene. Adapted from (Bankefors et al., 2011) [Color figure can be viewed at wileyonlinelibrary.com]

(http://cpu-smsd.com) is based on HR/MS and high-energy CID analysis in the negative ionization mode. The database is to date constituted by more than 4.000 saponins.

## 5.3 | Direct analysis in real time (DART) mass spectrometry

Beside MALDI-MS and LC-MS analyses, DART mass spectrometry has also been used to analyze saponins directly from raw materials such as plant tissues. One of the major issues when using DART for the screening of phytochemicals is the low ionization efficiency of DART for hydrophilic glycosides since the hydrophilic interaction between glycosides and the plant matrix molecules hinders the vaporization of ionized glycosides (Kim et al., 2014). In situ permethylation has been successfully applied by Kim et al. for the direct analysis of timosaponin AIII (**31**) from *Anemarrhena asphodeloides* Bunge rhizome. The powder was subjected to permethylation with tetramethylammonium hydroxide (25 wt.% in methanol) simultaneously with DART ionization. The detection of unfragmented permethylated timosaponin AIII (**31**), cationized by a trimethylammonium ion (Figure 13), was explained by the enhancement of volatility of permethylated compounds requiring ionization in less harsh DART conditions (Kim et al., 2014).

He *et al.* developed a solid-phase methylation of saponins using a stainless-steel methylation column (He et al., 2017). A stainless-steel column was filled with powdered NaOH in acetonitrile and DMSO saponin solutions containing 10% of methyl iodide were passed through the reaction column and collected in centrifuge tubes. The standard solutions, as well as the saponin

extracts from ginseng, were directly analyzed using DART-MS and $[M + H]^+$ or $[M + NH_4]^+$ ions of permethylated saponins were detected. Extensive fragmentations were observed during the ionization and mostly concerned glycosidic bond cleavages, cross-ring cleavages and methanol neutral losses (He et al., 2017).

6 | ION MOBILITY SPECTROMETRY FOR SAPONIN CHARACTERIZATION

Ion mobility mass spectrometry (IMS) is nowadays largely implemented amongst the MS-based methods for the structural analysis of biomolecules, with a special interest paid at large molecules such as proteins (Uetrecht et al., 2010) and nucleotides (Quinn et al., 2013). This methodology consists in the temporal separation of gaseous ions based on their mobility in a cell filled with a buffer gas under the influence of an electric field. IMS separates gaseous ions according to their ion mobility K, a physical quantity related to the ion charge (z) and collisional cross section (CCS) (Mesleh et al., 1996; Shvartsburg & Jarrold, 1996). As a first approximation, the CCS directly reflects the ion spatial structure. The drift time (t_D) of the ions across the mobility cell, that is, the measurand, is directly proportional to their CCS which reflects the three-dimensional shape of the ions in the gas phase (Gabelica & Marklund, 2018). IMS is then used to obtain direct information about the spatial structure of gaseous ions. To identify the 3D structure of gaseous ions, theoretical estimates of the CCSs (CCS_{th}) are computed based on atomistic computational simulations and directly compared to the experimental values (Gabelica & Marklund, 2018).
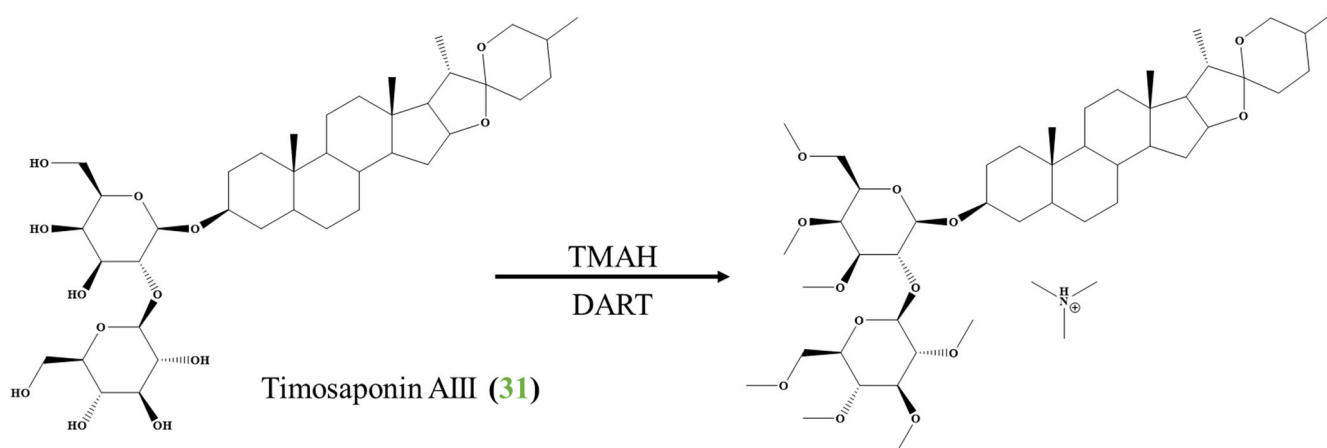
FIGURE 13 Molecular structures of the timosaponin AIII (**31**) and its permethylated homologue that appear as tetramethylammonium adduct upon DART analysis in presence of TMAH. Adapted from (Kim et al., 2014). DART, Direct analysis in real time; TMAH, tetramethylammonium hydroxide [Color figure can be viewed at wileyonlinelibrary.com]

We introduced IMS, using a traveling wave ion mobility mass spectrometer (TWIMS), in combination with molecular dynamics (MD) simulations for the structural analysis of saponins in 2017 and we focused on the saponins extracted from *H. forskali*, a sea cucumber abundantly observed around the Atlantic coasts of northwest Europe and in the Mediterranean Sea (Decroo et al., 2017). *H. forskali* contains 26 saponins in its Cuvierian tubules and 12 in its body wall (Decroo et al., 2017). Such a high diversity is assumed to be linked to a chemical defense mechanism, that is, the most commonly accepted biological role for these specialized metabolites. Holothuroid saponins are triterpene glycosides. The structure of the aglycone moiety, a holostanol (**10**), is derived from the tetracyclic triterpene lanosterol (**11**) in which the D-ring contains a γ-18(20)lactone (Decroo et al., 2017). The carbohydrate moiety is bound to the C3 of the aglycone and may include xylose (Xyl), glucose (Glc), quinovose (Qui), and 3-*O*-methylglucose (3-OMe-Glc) residues, as well as a sulphate group (Decroo et al., 2017).

As a typical example, isomeric holothurinoside C2 (**32**) and holothurinoside C (**33**) are linear 4-sugar saponins, respectively presenting the methylquinovose-glucose-glucose-xylose and the methylglucose-glucose-quinovose-xylose oligosaccharidic chains (Figure 14). These molecules are nicely separated by liquid chromatography with an elution time difference around 2 min and are readily distinguished using CID experiments (Decroo et al., 2017). However, in the IMS experiments, the corresponding $[M + Na]^+$ ions are characterized by quasi identical arrival times due to really similar $CCS = 256$ Å^2. Actually, these two isomeric saponins adopt quite similar gas phase structures upon ionization due to the collapse of the glycan and aglycone parts around the Na$^+$ ion, as shown in Figure 15.

Another striking observation made in that seminal study is that different gas phase ion structures may be created from a single molecular structure, i.e. a unique molecule, during the ionization process (Decroo et al., 2017). This is typically the case for the $[M + Na]^+$ ions of holothurinoside F (**34**) (Figure 14) that are detected with two different arrival times upon IMS, see Figure 16. Actually, holothurinoside F (**34**) is a branched 6-sugar saponin (Figure 14) with three and two monosaccharidic residues attached on the xylose residue. Upon Na$^+$ complexation, two different ion structures are base-line separated using IMS experiments as shown in Figure 16. In the most extended structure, only one part of the oligosaccharidic chain is in interaction with the sodium ion, whereas, in the most folded structure, the aglycone and both arms of the oligosaccharidic chain are interacting with the sodium ion (see Figure 16).

The principal conclusion of this initial study was that IMS experiments fail in discriminating saponin isomers presenting closely related structures, which is often the case when considering the extract from a natural source.

We further applied IMS together with MD simulations on a broad selection of saponin molecules covering a wide range of different structures in terms of the number of saccharide units and their topology, including linear and branched as well as monodesmosidic and bidesmosidic saponins (Decroo et al., 2019). We also investigated whether the selection of the cationization reaction, that is, yielding $[M + H]^+$, $[M + Na]^+$, and $[M + K]^+$, may affect the IMS results in terms of isomer separations. We showed that IMS may efficiently contribute to the structural characterization of saponins, since different saponin ions can present significantly distinct CCSs. Depending on the nature of the cation (in the positive ion mode), the differences in CCS can also be exacerbated, optimizing the gas-phase separation. However, we also concluded that the structural diversity and complexity of the saponins can definitively not be unraveled using IMS. The structural characterization of unknown saponins will be difficult to achieve based on IMS alone, even in combination with MD simulations.

We nevertheless obtained a nice result for the discrimination between monodesmosidic and bidesmosidic saponins. Actually, as shown in Figure 17, for the same number of monosaccharides, the $[M + Na]^+$ bidesmosidic ions are always significantly more compact than their $[M + H]^+$ homologues (about 10% reduction in CCS), whereas for the monodesmosidic molecules, the CCS are almost identical for the $[M + H]^+$ and $[M + Na]^+$ ions (Decroo et al., 2019). This difference is considered as a characterization criterion to distinguish monodesmosidic and bidesmosidic saponins. This was recently exploited for the follow-up of the microwave-assisted hydrolysis of the bidesmosidic saponins extracted from *C. quinoa* that produces monodesmosidic saponins by the specific hydrolysis of the ester bond at C28, see saponin B (**13**) in Figure 3 (Colson et al., 2020).

Regioisomeric and stereoisomeric saponins were recently successfully discriminated using ion mobility experiments, using a cyclic ion mobility (cIMS) setup with high ion mobility resolution (Colson et al., 2019). The cyclic TWIMS device is characterized by a scalable resolution, ranging from 65 (1 pass) upward depending on the number of passes/cycles (Giles et al., 2019). The IMS resolution increases with the square root of the number of passes (Giles et al., 2019).

As a model system, we selected the escin 1 (**35**) molecules extracted from the horse chestnut (HC) seeds that comprise isomeric saponins containing subtle differences such as cis-trans ethylenic configuration (stereoisomers) of a side chain or distinct positions of an acetyl group (regioisomers) on the aglycone, see Figure 18 for the escin 1 (**35**) family of isomers. For the $[M + Na]^+$ escin 1 (**35**)
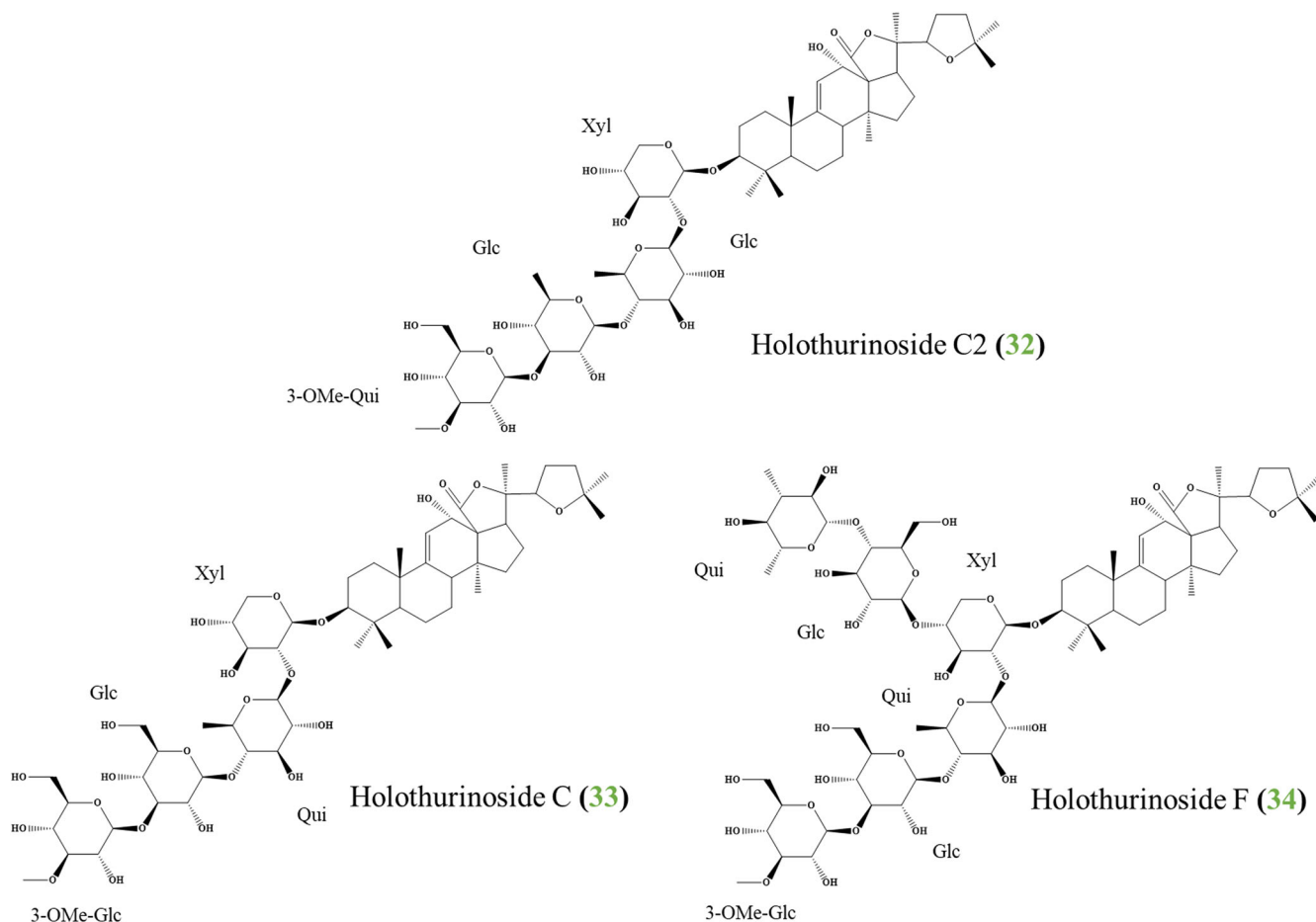
FIGURE 14 Molecular structures of isomeric four-sugar saponins holothurinoside C2 (**32**) and holothurinoside C (**33**) and six-sugar saponin holothurinoside F (**34**) extracted from *Holothuria forskali* (Decroo et al., 2017) [Color figure can be viewed at wileyonlinelibrary.com]
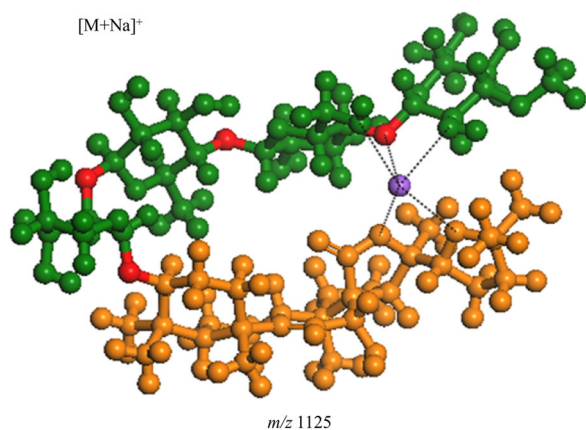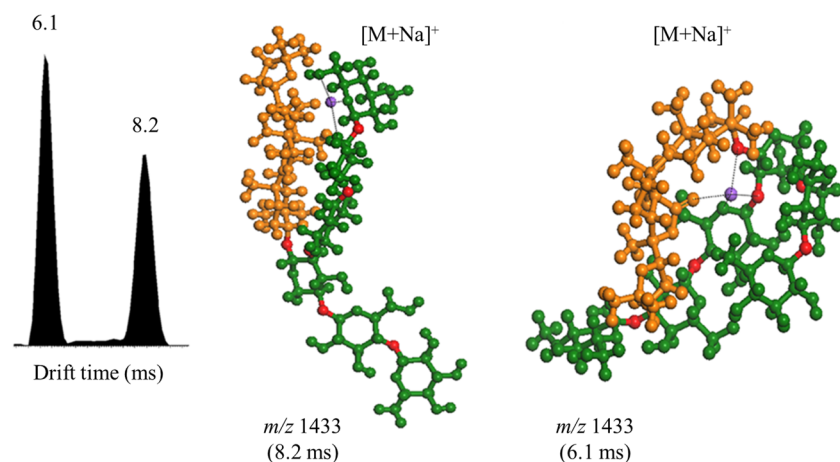

FIGURE 15 Molecular dynamics simulation of holothurinoside C (**33**) sodium adduct (m/z 1125) with the aglycone in orange, the glycan in green, the glycosidic bonds in red, and the Na^+ cation in purple. Adapted from (Decroo et al., 2017) [Color figure can be viewed at wileyonlinelibrary.com]

isomeric ions, small differences in the arrival time distribution (ATD) are monitored using a TWIMS when the isomeric saponins are first separated with liquid chromatography (Colson et al., 2019). The HC extract was further analyzed by direct infusion (no LC separation) on the cyclic ion mobility system. Whereas the $[M + Na]^+$ ions of the four escin 1 (**35**) isomers are not separated by cIMS with one pass, after fifteen passes, the ATD recorded upon direct infusion can be nicely deconvoluted into four different contributions, as presented in Figure 19.

7 | ON-TISSUE LOCALIZATION OF SAPONINS BY IMAGING METHODS

Direct visualization of saponins present in the plant or animal tissues represents an elegant method for assaying the biological activities of these glycosides. Matrix-assisted

FIGURE 16 LC-IMS analysis and molecular dynamic simulations of Holothurinoside F (**34**) sodium adducts (*m/z* 1433) with the aglycone in orange, the glycan in green, the glycosidic bonds in red, and the Na$^+$ cation in purple. Adapted from (Decroo et al., 2017) [Color figure can be viewed at wileyonlinelibrary.com]
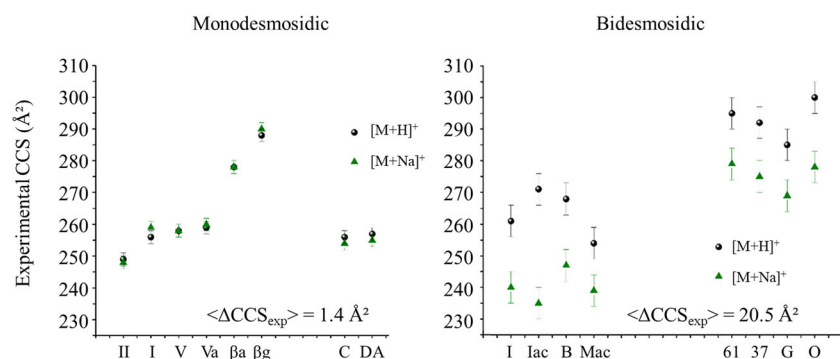

FIGURE 17 Comparison between measured CCS_{exp} of $[M + H]^+$ and $[M + Na]^+$ ions of monodesmosidic (left) and bidesmosidic (right) saponins with three and four saccharide units. Adapted from (Decroo et al., 2019) [Color figure can be viewed at wileyonlinelibrary.com]

laser desorption/ionization-mass spectrometry imaging (MALDI-MSI), also called MALDI Imaging, has undergone so many developments in the recent years (Amstalden van Hove et al., 2010), allowing it to be now used in many domains like clinical proteomics (Amstalden van Hove et al., 2010) or pharmaceutical fields (Amstalden van Hove et al., 2010). This procedure permits to detect and localize ions of interest directly on tissue sections and nearly without any preparation. MALDI imaging experiments performed on specialized metabolites start to be reported in the literature (Gadea et al., 2020), since the great added value of using MALDI-MS direct tissue analysis is to detect specific molecules in a spatially-resolved analysis. By this way, MALDI-MSI or MALDI profiling is recognized to open the door for important breakthroughs in the field of chemical ecology (Le Pogam et al., 2016). The localization of specialized secondary metabolites in an organism depends on their functional roles, as stated by McKey *et al.* who postulated that specialized metabolites are primarily allocated to organism parts of high fitness value, high risk of predation, or both (McKey, 1974).

MALDI-ToF-MSI has been used by Bai *et al.* to explore the distribution of ginsenosides (**29**) in the roots of *P. ginseng* with a special attention paid at the age of the plants (Bai et al., 2016). Actually, the establishment of *P. ginseng* age is economically relevant but remains difficult based only on the morphological appearance. Ginsenoside content increases with root age (Bai et al., 2016) and environmental variations (Bai et al., 2016), leading to higher prizes in the market. Also, ginsenosides (**29**) are classified into three common types depending on their aglycone, namely the 20(*S*)-protopanaxadiols (**40**), the 20(*S*)-protopanaxatriols (**41**), and the oleanolic acids (**42**) (Bai et al., 2016), see Figure 20. The pharmacological effects of different ginsenosides on the human body are significantly different depending on the molecular structures (Bai et al., 2016). LC-MS profiling of ginsenosides in root extract is the standard method to access the ginsenoside content of the roots (Bai et al., 2016).

Direct profiling of ginsenosides (**29**) on root cross sections definitively appears as a less time-consuming and more informative alternative of the standard extraction-based procedure. Using MALDI-ToF-MSI, Bai et al. detected 31 ginsenosides (**29**) with distinct localizations across the root cross sections. All the three types of ginsenosides (**29**) were successfully detected and visualized in images that nicely correlate with anatomical features. The *P. ginseng* at different ages were shown to be distinguishable based on the spatial distribution of the ginsenosides (**29**) (Bai et al., 2016). The different localization of protopanaxadiol-type (**40**) and protopanaxatriol-type ginsenosides (**41**) in the root was also
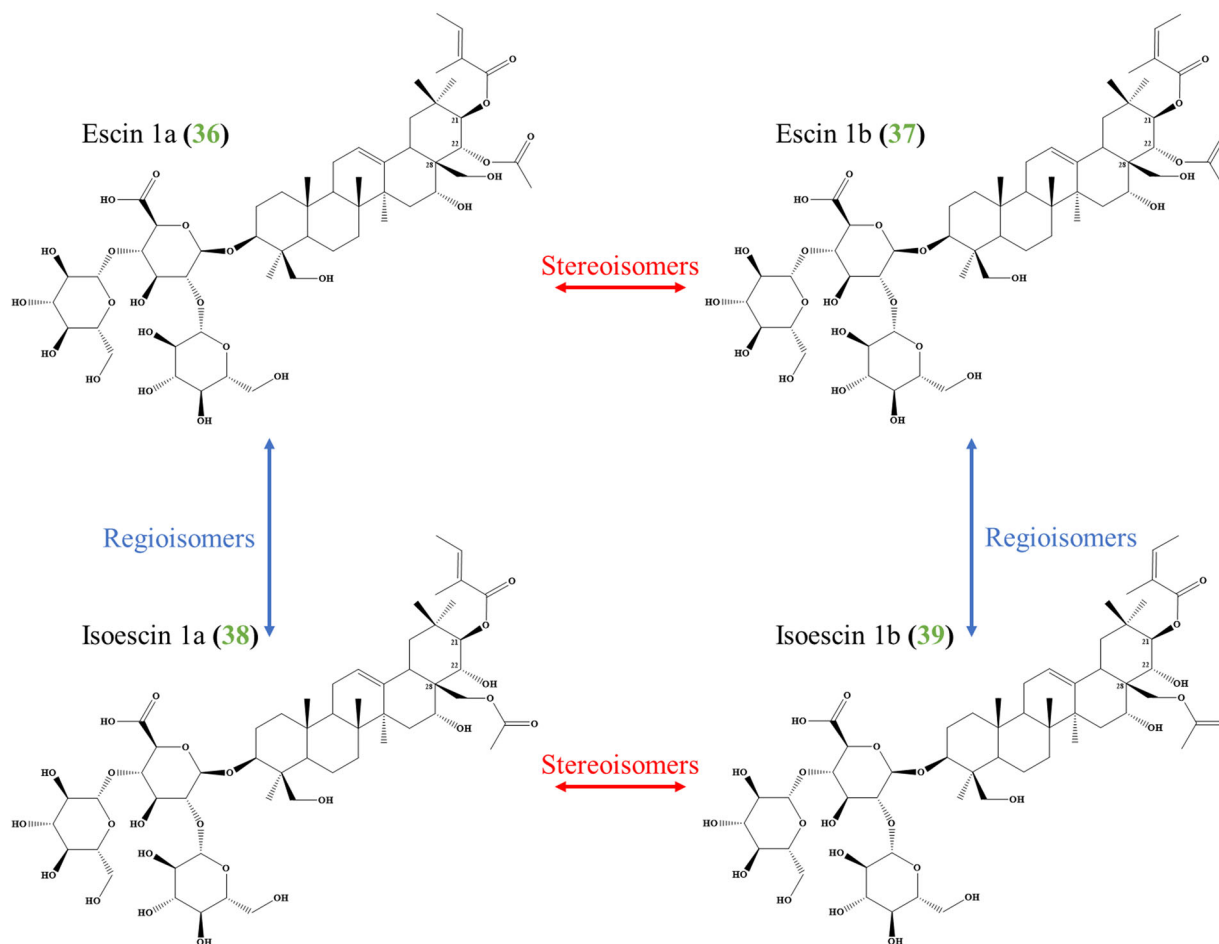
FIGURE 18 Nature of the isomeric relations between escin 1a (**36**), escin 1b (**37**), isoescin 1a (**38**), and isoescin 1b (**39**). Adapted from (Colson et al., 2019) [Color figure can be viewed at wileyonlinelibrary.com]
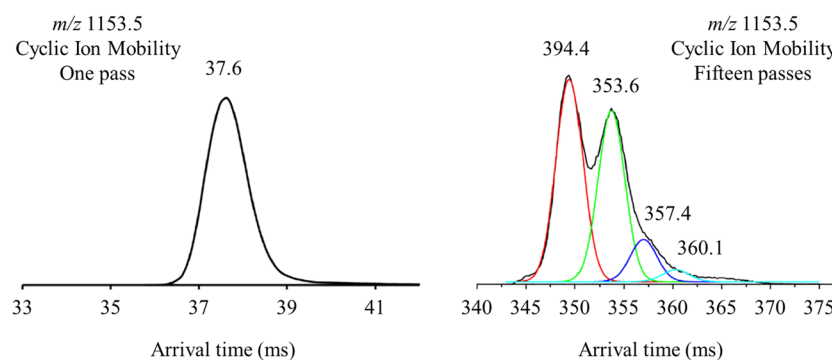

FIGURE 19 ESI-cIMS analyses (positive ion mode) by direct infusion of the HC extract—arrival time distribution for the $[M + Na]^+$ ions of the escin 1 (**35**) isomers (m/z 1153.5): comparison between one pass (left) and fifteen passes (right, deconvolution applied). Adapted from (Colson et al., 2019) [Color figure can be viewed at wileyonlinelibrary.com]

previously observed using MALDI-MSI by Taira et al. (2010) at a 100 μm resolution. Their analysis revealed that the ginsenosides are more concentrated in the lateral roots and are preferentially located toward the outer portion and the tip of the lateral roots (Taira et al., 2010). Desorption electrospray ionization mass spectrometry imaging (DESI-MSI)

has also be used for studying the ginsenosides (29) localization in the ginseng main and branch roots (Yang et al., 2021), indicating a tissue specific localization of the ginsenoside (**29**) congeners (Yang et al., 2021).

The rhizome of *Glycyrrhiza glabra* (licorice) was analyzed by high-resolution mass spectrometry imaging
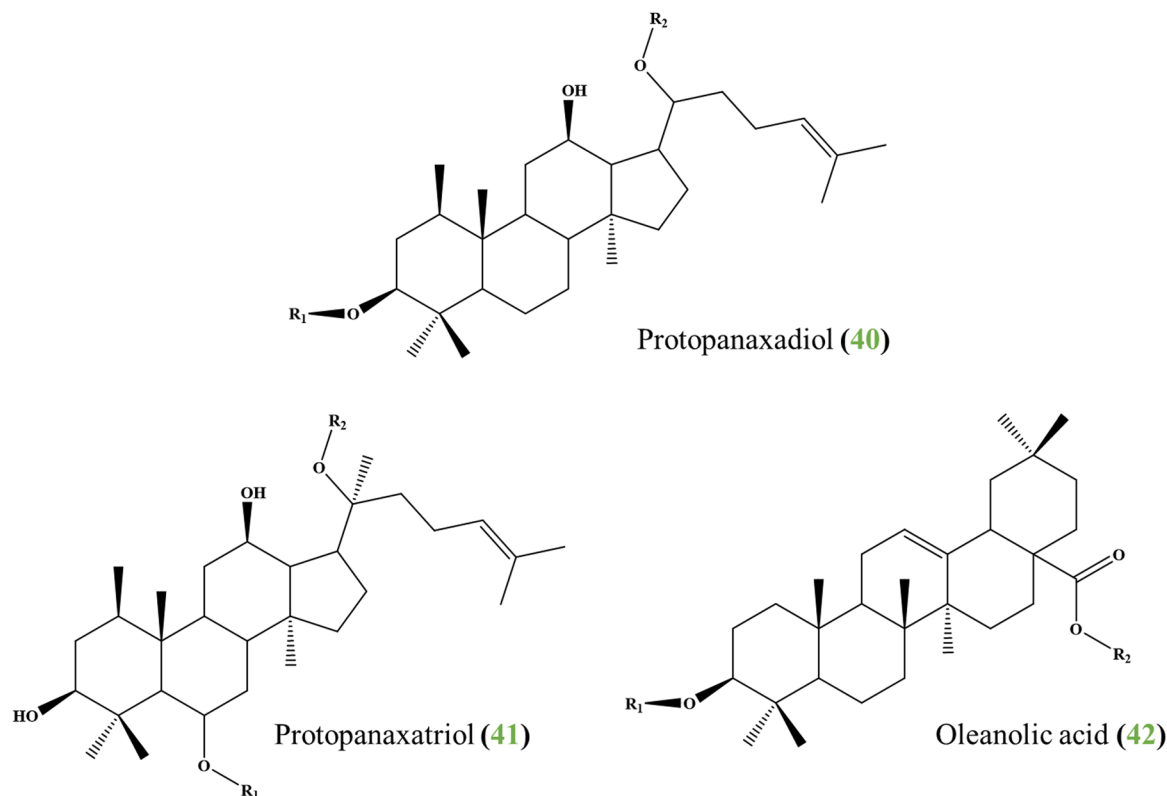
FIGURE 20 Molecular structures of the three common aglycones of the ginsenosides (**29**): 20(*S*)-protopanaxadiols (**40**), the 20(*S*)-protopanaxatriols (**41**), and oleanolic acids (**42**) (Bai et al., 2016) [Color figure can be viewed at wileyonlinelibrary.com]

and tandem mass spectrometry imaging using atmospheric pressure matrix-assisted laser desorption/ionization coupled to a high resolution orbitrap analyzer (Li et al., 2014).

In this study, Li et al. focused on different families of active compounds, including flavonoids, chalcones, isoflavanes and triterpene saponins. Glycyrrhizic acid (**43**) and licorice saponins G2 (**44**), B2 (**45**), and J2 (**46**) are the major saponins found in licorice (Figure 21) (Li et al., 2014). Interestingly, the $[M + Na]^+$ ions of **44** (*m/z* 861.38793) and the $[M + K]^+$ ions of **43** (*m/z* 861.36695) are isobaric with a mass difference of only 0.021 Da (Figure 21), requiring a high resolution analyzer for their discrimination.

Figure 22 presents a mass spectrum from a rhizome cross section in the corresponding mass window revealing the coexistence of the $[LS\ G2 + Na]^+$ ions and the $[GA + K]^+$ ions. Figure 22 also reveals that the spatial distributions of licorice saponin G2 (**44**) and glycyrrhizic acid (**43**) are strongly different across the rhizome (Li et al., 2014) (Figure 22).

Back to the marine animal saponins, we investigated using MALDI-MSI the role of the holothuroid triterpene glycosides in the chemical defense mechanisms of the sea cucumber *H. forskali* (Van Dyck et al., 2011). Using

MALDI direct tissue analysis of a body wall tissue section, we identified 8 major saponin ions, namely holothurinoside C (**33**) (*m/z* 1125), desholothurin A (12) (*m/z* 1141), holothurinoside E (**47**) (*m/z* 1287), holothurinoside A (**48**) (*m/z* 1303), holothurinoside F (**34**) (*m/z* 1433), holothurinoside G (**49**) (*m/z* 1449), holothurinoside H (**50**) (*m/z* 1463), and holothurinoside I (**51**) (*m/z* 1479) as $[M + Na]^+$ ions (Van Dyck et al., 2011), see Figure 14 for selected molecules. As shown in Figure 23, these saponins showed specific localizations within the body wall cross section with the saponins being mainly localized in the mesothelium (inner part of the body wall) for the relaxed animals. When the living animals were submitted to a smooth stress period (turning soft balls) before euthanasia, the MALDI-MSI profile was observed to be significantly affected, see Figure 23. The saponins have migrated toward the external part of the body wall, the so-called epidermis, and some of them, typically *m/z* 1287 and 1303, were even no longer detected, suggesting their release in the surrounding water for chemical defense (Van Dyck et al., 2011).

Several species of sea cucumbers of the family Holothuriidae, particularly *H. forskali*, possess a particular mechanical defense system, called the
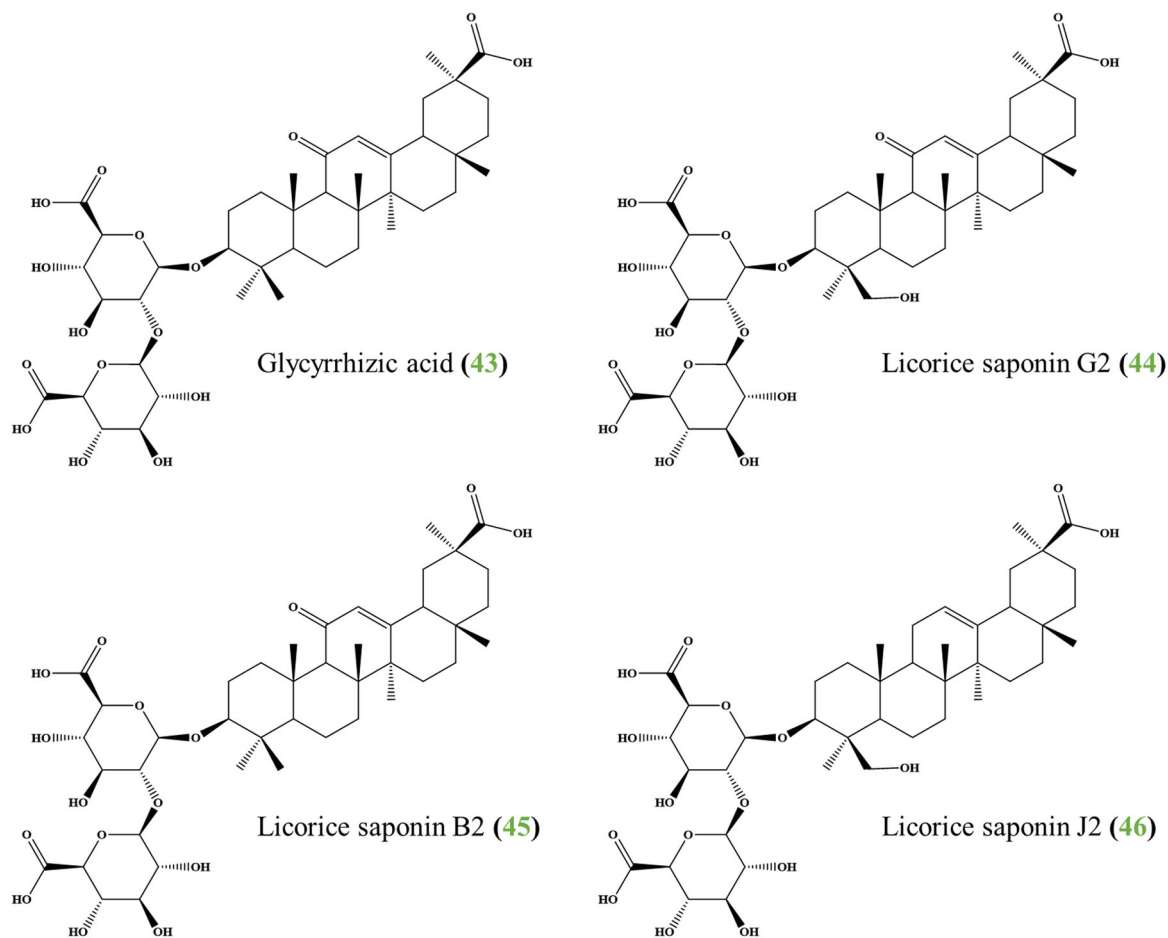
FIGURE 21 Molecular structures of the four major saponins found in licorice: glycyrrhizic acid (**43**) and licorice saponin G2 (**44**), licorice saponin J2 (**45**), and licorice saponin B2 (**46**) (Li et al., 2014) [Color figure can be viewed at wileyonlinelibrary.com]
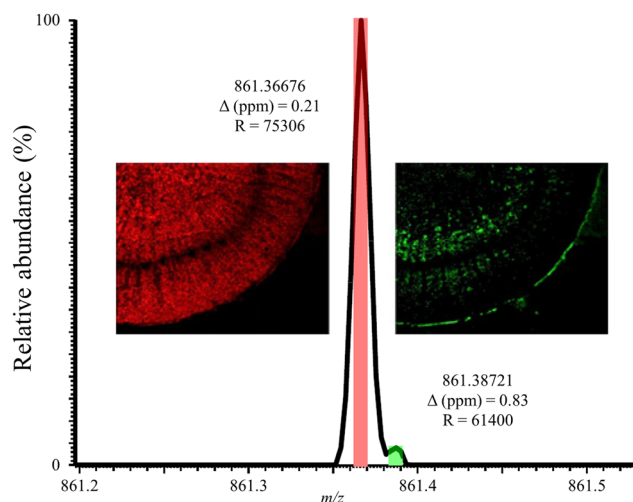
FIGURE 22 MALDI-MSI analysis (positive ion mode) of the rhizome cross section showing the coexistence and the spatial distributions of [LS G2 + Na]$^+$ and [GA + K]$^+$ions. Adapted from (Li et al., 2014) [Color figure can be viewed at wileyonlinelibrary.com]

Cuvierian tubules (Van Dyck, Gerbaux, et al., 2010). It was demonstrated that these organs are characterized by a highly concentrated cocktail of specific saponins (Van Dyck, Gerbaux, et al., 2010). Using MALDI-MSI, the precise localization of these saponins across the Cuvierian tubules has been investigated with a special attention paid at the stress/unstress state of the animals, before the euthanasia. Again, a differential composition in saponins depending on the condition of the animal has been detected and detection of variations in the saponin content at the molecular level was made possible using MALDI-imaging (Van Dyck, Gerbaux, et al., 2010). The same type of analysis was carried out on the sea star *A*steria rubens and allowed us to obtain information on the distribution of saponins within different organs. MALDI-MSI performed at different spatial resolutions revealed that the inter- and intra-organ distributions of saponin congeners are not homogeneous (Demeyer et al., 2015).
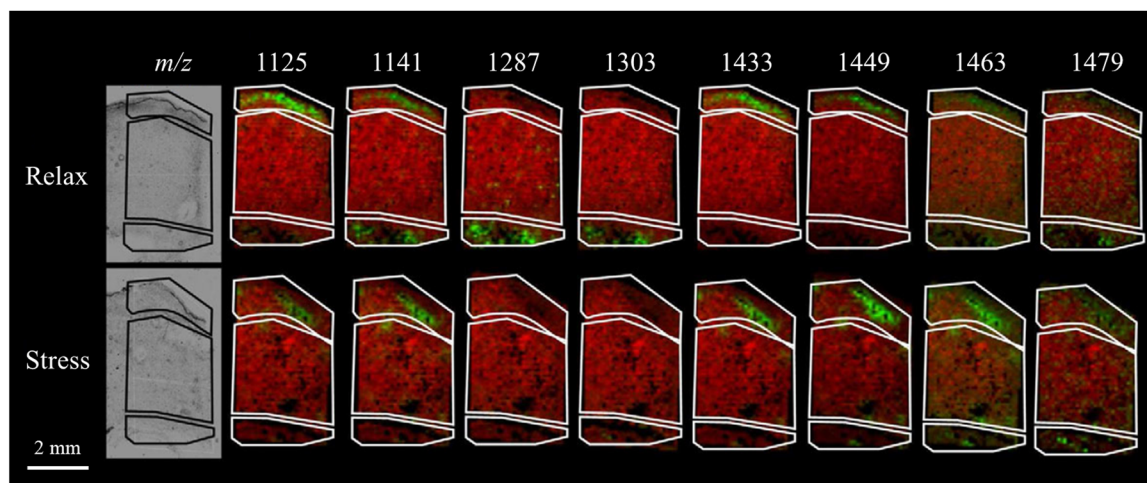
FIGURE 23 Molecular images pointing the localization of saponin ions (in green) in the body wall sections (epidermis on the top, dermis in the middle and mesothelium on the bottom) obtained by MALDI-MSI on relaxed (above) and stressed (below) *Holothuria forskali*: holothurinoside C (**33**), desholothurin A (**12**), holothurinoside E (**47**), holothurinoside A (**48**), holothurinoside F (**34**), holothurinoside G (**49**), holothurinoside H (**50**), and holothurinoside I (**51**). Adapted from (Van Dyck et al., 2011) [Color figure can be viewed at wileyonlinelibrary.com]

8 | QUANTITATIVE ANALYSIS OF SAPONINS

The previous sections reveal that mass spectrometry methods have nowadays reached a sufficiently high degree of maturity to allow identifying saponins in plant and animals extracts, as well as directly on tissue by imaging methods. This is all the more remarkable that most of the time saponins occur as a multicomponent mixture with similar structures and polarities. As an additional typical example, more than fifty oleanane-type triterpene (**52**) saponins were detected and identified in the *Camellia sinensis* seed extracts (Wu et al., 2019).

Although saponin extracts have been shown to present a broad spectrum of biological properties and application potentials, validated methods are lacking to provide full quantitative analysis for saponins in extract. Actually, saponin quantification remains challenging due to the lack of reference molecules such as isotopic labelled internal standards (ISs) or even pure saponins. This is often the case for many phytochemicals whose quantification remains challenging.

Generally, the total saponin content within an extract is determined using indirect methods such as the vanillin-sulfuric acid assay (Le et al., 2018), the orcinol reaction assay (Dai et al., 2020) or the measure of the hemolytic activity (Habicht et al., 2011). The vanillin-sulfuric acid assay is the most common spectrophotometric method for saponin quantification since it is simple and fast to operate (Le et al., 2018). This procedure starts from an acidic hydrolysis to release the free aglycones that further react with vanillin to produce a brown chromophore that is quantified using UV-vis spectrophotometry (450 nm). However, this method can only measure the total saponin content and is not specific enough. For the orcinol reaction, upon acidic hydrolysis in harsh conditions, the released monosaccharides are ultimately converted by dehydration in furfural derivatives that react with the Bial reagent (orcinol, HCl and FeCl$_3$) generating a blue chromophore whose concentration is determined using spectrophotometry methods (540 nm) (Dai et al., 2020). Interestingly, the vanillin-sulfuric acid and the orcinol assays may appear complementary since they target the aglycone and the glycan parts of the saponin molecules, respectively. However, discrepancies may be encountered since both assays are affected by bias such as the non-specificity of the vanillin assay and the coexistence of hexose and pentose in the polysaccharidic chains whose dehydration products are different (Le et al., 2018; Dai et al., 2020). Also, the orcinol assay do not considered the coexistence of saponin molecules presenting a different number of monosaccharidic residues (Dai et al., 2020; Van Dyck, Flammang, et al., 2010).

The total saponin content is often estimated based on the determination of the hemolytic activity of the extracts, that is, the propensity to cleave the erythrocyte cell membranes releasing hemoglobin in the extracellular medium (Kalinin et al., 1996; Mackie et al., 1968). The measurement of the hemolytic activity of the saponin extracts thus reflects the effectiveness of the saponin mixture to lyse erythrocytes. The quantification of the hemolytic activity is based on the determination of the free hemoglobin concentration by spectrophotometry at

540 nm (Mackie et al., 1968). The spectrophotometric measurements are converted to milligram equivalents of plant saponins by gram of extract, using a standard curve prepared with a reference saponin extract. This method neglects that differences in saponin structures may affect their hemolytic activity (Van Dyck, Flammang, et al., 2010).

Coupling liquid chromatography to mass spectrometry and photo-diode array detector respectively affords qualitative and quantitative data for the characterization of phytochemicals such as flavonoids, for instance (Chen et al., 2012). At variance with saponins, numerous flavonoids are commercially available and standard solutions can then be prepared for quantitative measurements. Moreover, saponins show very weak absorbance in the short wavelength range (<210 nm) rendering sensitive detection by ultraviolet spectroscopy almost impossible. Liquid chromatography ultraviolet analysis of saponins result in a high level of baseline, limiting the choice of solvents and the use of mobile phase modifiers for improved separation (Ha et al., 2006). As a striking example, Wu et al. used ultra-performance liquid chromatography diode array detection mass spectrometry (UPLC-DAD-MS) for the qualitative and quantitative analysis of the saponins extracted from the *C. sinensis* seeds (Wu et al., 2019). They first isolated theasaponin E1 (53) from tea seeds and used it as reference standard for their UV detection at 210 nm (Wu et al., 2019). They compared the LC-MS and LC-DAD profiles of the crude extract, obtained by refluxing the biomass in 70% methanol, and a saponin-enriched extract, obtained by consecutive extractions with different polar solvents (petroleum ether, ethyl acetate, 1-butanol). Their analysis reveals that, whereas the LC-MS profile is almost insensitive to the purity of the extracts, the LC-DAD measurement is more applicable for detecting saponins at higher concentrations. The second disadvantage of this method is that all saponins are quantified by a unique standard substance that is moreover used as an external standard since it belongs to the extracted saponins. Recently, we have qualitatively and quantitively characterized the saponins extracted from the *C. quinoa* husks (Quinoa extract [QE]) only using LC-MS experiments (Colson et al., 2020). We introduced hederacoside C (54) (Sigma-Aldrich) as an IS to determine the mass proportions of all the saponins detected in the quinoa extract. hederacoside C (54) is extracted from the *Hedera helix* leaf and therefore is not present in the QE (Havlíková et al., 2015). The molar proportion (% in the quinoa husk extract) and the mass fraction (mg/g of the quinoa husk powder) of each saponin was estimated based on the ion signal ratios as determined by LC-MS experiments.

Astragaloside IV (55) is one of the major ingredients present in the *Astragali Radix*, the root of Astragalus, that is an important medical herb used in traditional Chinese medicine (Kafle et al., 2020). Due to the availability of astragaloside IV (55), Kafle et al. succeeded in developing a robust quantitative method based on the standard addition method. Quantification by standard addition provides an intrinsic correction of ion suppression or ion enhancement upon LC-MS. This method provides better accuracy and can be used in the absence of an isotopic labelled IS (Colson et al., 2020; Kafle et al., 2020). Ha et al. developed a quantitative and qualitative method for the determination of saponins in Platycodi Radix by coupling liquid chromatography to mass spectrometry for the qualitative dimension and to evaporative light scattering detection for the quantitative aspect (Ha et al., 2006). The method has been validated for linearity, accuracy and limit of detection (LOD). The linearity was established for the ten analyzed saponins on the 0.3–20 µg range with a LOD around 0.15 µg (Ha et al., 2006).

Zhang et al. (2015) used LC-MS/MS to simultaneously analyze 5 steroid saponins in rat plasma. The quantification was achieved using MRM experiments in the positive ion mode and selecting gingenoside RB$_1$ (56) as the IS. The selection of the IS was made based on its high extraction efficiency and its chromatographic retention time similar to the analytes. The MRM strategy was built on the a priori determined major sensitive transitions for each of the $[M + H]^+$ precursor ions and all correspond to sugar losses. MRM experiments were also advantageously implemented by Liu et al. (2015) to investigate the tissue distribution of six major saponins present in rats after oral administration of Zhenqi Fuzheng capsules. Again, the quantification was performed using low-energy collision CID in MRM scan modes using precursor ion→product ion transitions established based on CID experiments performed on standard molecules. Hesperedin (57) was used as the IS. This study reveals that the saponin tissue concentrations decrease from spleen>stomach>thymus>lung>liver>kidney>heart>testicle.

Quantification of saponins within an extract remains challenging and when analyzing saponin extracts with MS-based methods, handling the data remains problematic for the comprehensive report of the results, but also for their efficient comparison. Often, identified saponins are compiled in tables presenting all molecules together with, at least, their molecular masses, their chemical compositions, and the mass-to-charge ratios of the corresponding ions. These tables, however, are usually difficult to read and interpret. We therefore introduced a representation in sector diagrams to combine, in a single graph, the data generated by MALDI, LC-MS and ion mobility experiments (Decroo et al., 2017). For a given extract, MALDI-ToF or LC-MS analyses (together with HRMS measurements) are used to identify the

different saponin elemental compositions that are characterized by their m/z ratio and their relative abundances (as measured on the basis of peak intensities or LC signal integration). For the calculation of relative abundances, all isotopic signals are to be considered. If a saponin molecule appears with different cationization, that is, $[M + H]^+$ and $[M + Na]^+$, the ion intensities are added. At a second level of description, the LC-MS data are used to characterize within each elemental composition (m/z ratio), the isomeric diversity. This is done by using the retention time and the relative peak integration. Finally, for each of the retention time, the ion mobility data (including the relative peak integration measured from the ATD) is added to identify coeluting isomeric saponins or catiomers. All those data are compiled within sector diagrams presenting different areas corresponding to the different identified elemental compositions. The surfaces are labeled according to the m/z ratio of the detected ions. In the diagram, the inner concentric circle represents the LC-MS data, whereas the outer circle presents the ion mobility experiment data (Decroo et al., 2017). As for a typical example, we analyzed the saponins extracted from different organs of *H. forskali*, namely the body wall, the gonads and the Cuvierian tubules, using MALDI-MS, LC-MS/MS, and LC-IMS (Decroo et al., 2017). We detected 10, 16, and 22 different saponins, that are four-, five-, and six-sugar saponins, within the body wall, gonads, and Cuvierian tubules. Each organ was shown to contain a specific cocktail of saponins as exemplified for the four-sugar saponins in Figure 24. A quick look at the comparison between the three sector diagrams reveals that (i) two different saponin compositions are present and detected at m/z 1125 and 1141 for the $[M + Na]^+$ ions, (ii) that the relative abundances of these compositions is organ dependent, and (iii) that the m/z 1125 saponin is unique in the body wall, whereas one and two additional isomers are detected in the gonads and the Cuvierian tubules, respectively. This data integration is useful for data interpretation since it allows for a direct and fast comparison, both in terms of composition and relative proportion of the saponin contents in different extracts (Decroo et al., 2017).

As a direct application of this representation, we demonstrated that the microwave-assisted hydrolysis of the bidesmosidic saponins extracted from the Quinoa Husk is quantitative by the direct comparison between the sector diagrams built for the natural extracts and the hydrolyzed one (Colson et al., 2020).

Indeed, as shown in Figure 25, saponin O (**58**) is a [3 + 1] bidesmosidic saponin presenting a hydrolyzable ester function at C28, whereas the principal trisaccharidic chain is appended at C3 via an acetal function. Upon microwave heating at pH 10, 150°C for 5 min, saponin O^h (**59**), the monodesmosidic counterpart molecule, is generated as demonstrated using mass spectrometry. The sector diagram presented in Figure 26a reveals that four [3 + 1] saponins are detected at m/z 1113, 1127, 1141, and 1157 from the natural extract, with the m/z 1157 saponin being the most abundant. After the microwave-assisted hydrolysis, the [3 + 1] saponins have totally disappeared and are quantitively converted into their [3 + 0] counterparts as shown in the second sector diagram of Figure 26B. It is important to note that the relative proportions between the two sets of saponins, natural and hydrolyzed, have remained constant, indicating that the hydrolysis is quantitative for the four molecules (Colson et al., 2020).

9 | MISCELLANEOUS

Saponin-rich plant extracts are often prescribed in traditional medicine preparations due to their anti-inflammatory, anti-hepatotoxic, and immunostimulant activities (Moghimipour & Handali, 2015). Based on the concept that protein-ligand interactions are involved in numerous biological processes, including drug-related medicinal activities, the investigation of ex situ protein-ligand complexes are of extreme
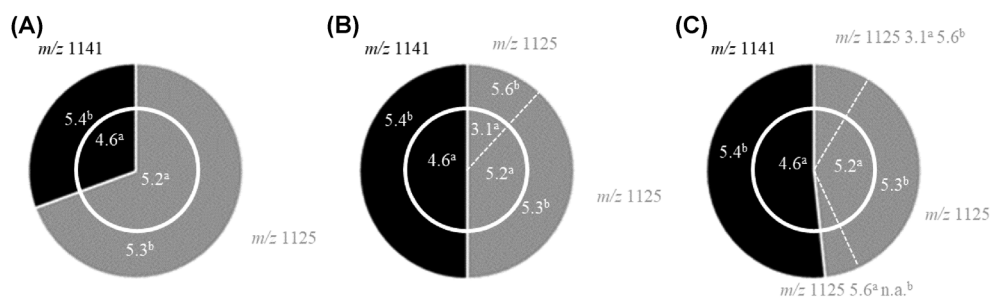
FIGURE 24 Compilation of MALDI-ToF-MS, LC-MS/MS and LC-IMS analyses permitting to establish the distribution of the four-sugar saponins (m/z 1125 and 1141) in body wall (A), gonads (B), and Cuvierian tubules (C) with the retention times ([a], min) and drift times ([b], ms; n.a., not attributed). Adapted from (Decroo et al., 2017) [Color figure can be viewed at wileyonlinelibrary.com]
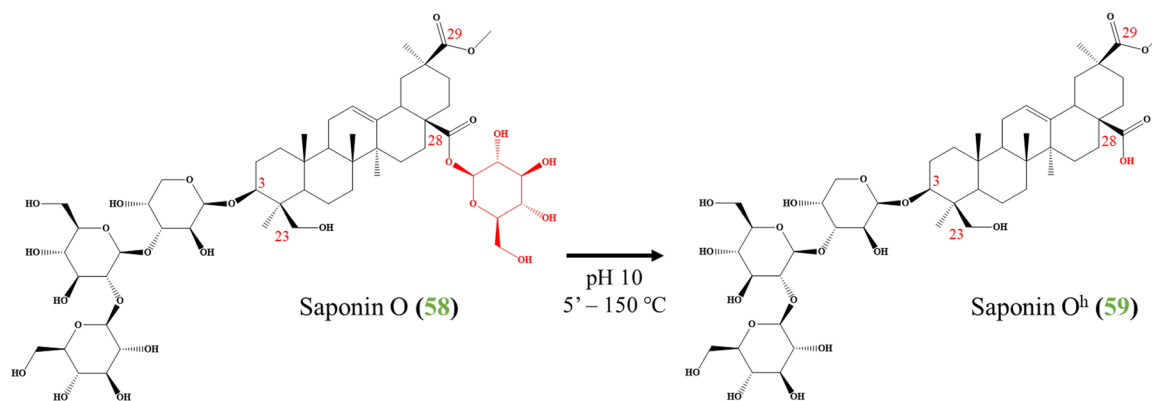
FIGURE 25 Microwave-assisted hydrolysis of saponin O (**58**), extracted from *Chenopodium quinoa*, to saponin O[h] (**59**). Adapted from (Colson et al., 2020) [Color figure can be viewed at wileyonlinelibrary.com]
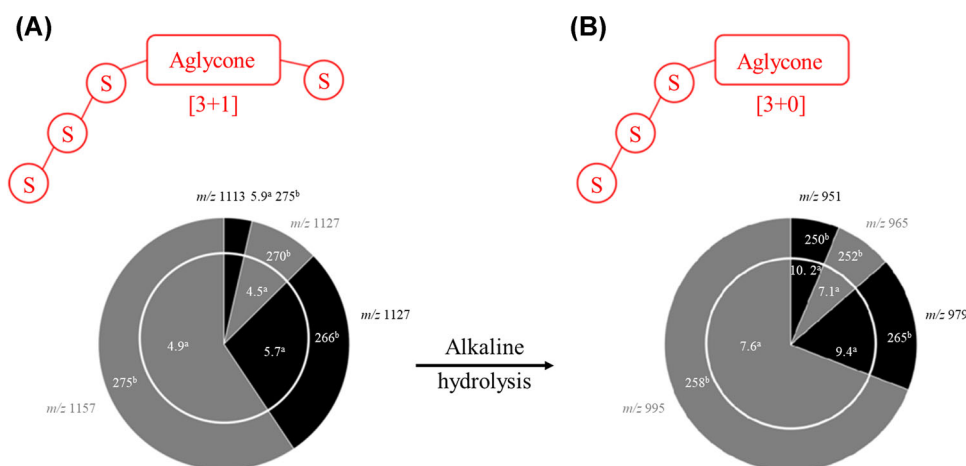

FIGURE 26 Compilation of MALDI-ToF-MS, LC-MS/MS and LC-IMS analyses permitting to establish the composition of the [3 + 1] saponins from *Chenopodium quinoa* (A) and the composition of the [3 + 0] saponins generated by the microwave-assisted hydrolysis (B) with retention times ([a], min) and collisional cross section ([b], Å[2]), showing a quantitative and nonspecific hydrolysis (pH 10, 150°C, 5 min). Adapted from (Colson et al., 2020) [Color figure can be viewed at wileyonlinelibrary.com]

importance to decipher the role of small therapeutic molecules against different pathologies (Barczyk et al., 2005). Cytochrome *c* (Cyt) is one of the deeply characterized proteins and often serves as a model protein for the study of ligand-protein complexes (Barczyk et al., 2005).

The noncovalent complexes of cytochrome *c* (Cyt) and ginsenosides (**29**) have been studied using electrospray Ionization mass spectrometry (ESI-MS) and 1:1 and 1:2 complexes between cytochrome *c* (Cyt) and several ginsenosides (**29**) have been detected (Zhang et al., 2007). The dissociation constants of the 1:1 and 1:2 complexes have been determined based on titration experiments by ascribing the ion abundances to the ion solution concentrations, as it is often performed when studying ligand-protein interactions using ESI-MS (Zhang et al.,

2007). They further evaluated the interactions of ginsenosides (**29**) and amino acids (AA) using ESI-MS and 1:1 and 2:1 noncovalent complexes of ginsenosides (**29**) and amino acids (AA) were observed in the mass spectra. Based on the determined dissociation constants, they concluded that the acidic and the basic amino acids, more strongly bind to cytochrome *c* (Cyt) than other amino acids. This was further corroborated using theoretical calculations that reveal that H bond interactions are responsible for the stabilization of the detected complexes (Qu et al., 2009).

In 2012, Liu et al. investigated the noncovalent interactions between cytochrome c (Cyt) and several saikosaponins a (**60**) and c (**61**) (Figure 27) extracted from *Bupleurum falcatum*. They first explored the binding propensity of
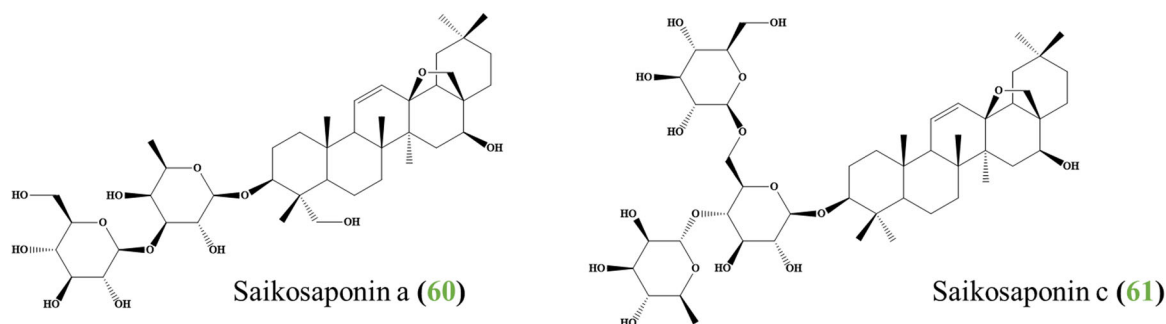
FIGURE 27 Molecular structures of saikosaponin a (**60**) and saikosaponin c (**61**) (Liu et al., 2012) [Color figure can be viewed at wileyonlinelibrary.com]
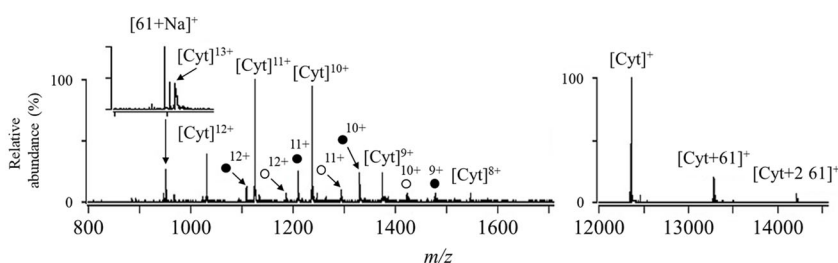
FIGURE 28 ESI-MS analysis (positive ion mode) showing the multiply charged complexes of cytochrome *C* (Cyt) with Saikosaponin c (**61**) where ● represents the 1:1 noncovalent complexes and ○ represents the 1:2 noncovalent complexes, each with their respective state of charge. Adapted from (Liu et al., 2012) [Color figure can be viewed at wileyonlinelibrary.com]

saikosaponins a (**60**) or c (**61**) with cytochrome *c* (Cyt) and detected 1:1 and 1:2 noncovalent complexes (Liu et al., 2012), see Figure 28. Interestingly, they also separately monitored the noncovalent interactions between saponin fragments, that is, oligosaccharide and aglycone, to get insight into the structure-binding relationship of saponins with **Cyt** (Liu et al., 2012). Doing so, no complex ions between triterpenes and **Cyt** were detected, whereas similar dissociation constant (Kd) values were obtained for the **Cyt** complexes of saikosaponins or their fragment oligosaccharides. They hypothesized that the saponin glycosyl moiety represents the effective interaction group with **Cyt** and they proposed that saikosaponins and saccharides interact with **Cyt** by hydrogen bonds (Liu et al., 2012) (Figure 28).

10 | CONCLUSIONS

In the present review, we explored the many different possibilities offered by mass spectrometry for the investigation of saponins. Saponins are specific metabolites present in plants and animals that mostly fulfill defensive roles, even if they are nowadays presumed to play significant roles in the intra and interspecies communications. Saponins are natural glycosides formally arising from the condensation of a saccharide chain—the glycan—onto a lipophilic triterpene—the aglycone. The saponin family of molecules is characterized by such an extreme structural diversity that their structural characterization remains difficult.

Mass spectrometry methods are constantly being developed to allow the study of biological systems at the molecular level. The study of saponins obviously benefits from all these developments which allow for a possible characterization of saponins within enriched extracts and directly on tissues. Basically, most of the structural characterization MS-based methods have been applied on saponin ions, including GC-MS, LC-MS, MALDI-MS, accurate mass measurements, CID, ion mobility experiments, MALDI-imaging, DESI-MS, DART-MS and native mass spectrometry for the investigation of saponin/protein interactions.

Whatever the current successes of the characterization of saponins by mass spectrometry, several aspects remain problematic. First of all, from a structural point of view, one of the current challenges concerns the establishment of the stereochemistry of the different stereogenic centers present in saponins, including the glycosidic bond configurations and the discrimination between epimeric sugars. It is likely that the development of the capabilities of

ion mobility experiments, in combination with multistep CID experiments may afford nice pieces of information. The complementarity between IMS and CID represents one of our research subjects nowadays, in conjunction with theoretical chemistry.

The development of efficient and sensitive methods for the study of saponins and specific metabolites in general is a prerequisite for the establishment of their structure/activity relationship for understanding their biological in vivo roles, but also for securing their applications in pharmaceutical applications.

ACKNOWLEDGMENTS

REFERENCES

Adinolfi M, Mangoni L, Marino G, Parrilli M, Self R. Fast atom bombardment mass spectrometry of the muscarosides. An aid to the glycoside sequence determination. *Biol. Mass Spectrom.* 1984; *11*: 310–314.

Amstalden van Hove ER, Smith DF, Heeren RMA. A concise review of mass spectrometry imaging. *J. Chromatogr. A.* 2010; *1217*: 3946–3954.

Arabski M, Węgierek-Ciuk A, Czerwonka G, Lankoff A, Kaca W. Effects of saponins against clinical *E. coli* strains and eukaryotic cell line. *J. Biomed. Biotechnol.* 2012; : 1–6.

Augustin JM, Kuzina V, Andersen SB, Bak S. Molecular activities, biosynthesis and evolution of triterpenoid saponins. *Phytochemistry* 2011; *72*: 435–457.

Bahrami Y, Franco C. Structure elucidation of new acetylated saponins, lessoniosides A, B, C, D, and E, and non-acetylated saponins, lessoniosides F and G, from the viscera of the sea cucumber *Holothuria lessoni. Mar. Drugs.* 2015; *13*: 597–617.

Bahrami Y, Zhang W, Chataway T, Franco C. Structural elucidation of novel saponins in the sea cucumber *Holothuria. Mar. Drugs.* 2014; *12*: 4439–4473.

Bahrami Y, Zhang W, Franco C. Discovery of novel saponins from the viscera of the sea cucumber *Holothuria lessoni. Mar. Drugs.* 2014; *12*: 2633–2667.

Bai H, Wang S, Liu J, Gao D, Jiang Y, Liu H, Cai Z. Localization of ginsenosides in *Panax ginseng* with different age by matrix-assisted laser-desorption/ionization time-of-flight mass spectrometry imaging. *J. Chromatogr. B.* 2016; *1026*: 263–271.

Bankefors J, Broberg S, Nord LI, Kenne L. Electrospray ionization ion-trap multiple-stage mass spectrometry of *Quillaja saponins. J. Mass Spectrom.* 2011; *46*: 658–665.

Barczyk K, Kreuter M, Pryjma J, Booy EP, Maddika S, Ghavami S, Berdel WE, Roth J, Los M. Serum cytochrome c indicatesin vivo apoptosis and can serve as a prognostic marker during cancer therapy. *Int. J. Cancer.* 2005; *116*: 167–173.

Bondoc KGV, Lee H, Cruz LJ, Lebrilla CB, Juinio-Meñez MA. Chemical fingerprinting and phylogenetic mapping of saponin congeners from three tropical holothurian sea cucumbers. *Comp. Biochem. Physiol. Part B Biochem. Mol. Biol.* 2013; *166*: 182–193.

Budzikiewicz H, Wilson JM, Djerassi C. Mass spectrometry in structural and stereochemical problems. XXXII. Pentacyclic triterpenes. *J. Am. Chem. Soc.* 1963; *85*: 3688–3699.

Burnouf-Radosevich M, Delfel NE, England R. Gas chromatography-mass spectrometry of oleanane- and ursane-type triterpenes—Aapplication to *Chenopodium quinoa* triterpenes. *Phytochemistry.* 1985; *24*: 2063–2066.

Campagnuolo C, Fattorusso E, Taglialatela-Scafati O. Feroxosides A-B, two norlanostane tetraglycosides from the Caribbean sponge *Ectyoplasia ferox. Tetrahedron.* 2001; *57*: 4049–4055.

Caulier G, Flammang P, Gerbaux P, Eeckhaut I. When a repellent becomes an attractant: Harmful saponins are kairomones attracting the symbiotic Harlequin crab. *Sci. Rep.* 2013; *3*: 1–5.

Caulier G, Flammang P, Rakotorisoa P, Gerbaux P, Demeyer M, Eeckhaut I. Preservation of the bioactive saponins of *Holothuria scabra* through the processing of trepang. *Cah. Biol. Mar.* 2013; *54*: 685–690.

Chaieb I. Saponins as Insecticides: A Review. *J. plant. Prot.* 2017; *5*: 39–50.

Chen J, Guo X, Song Y, Zhao M, Tu P, Jiang Y. MRM-based strategy for the homolog-focused detection of minor ginsenosides from notoginseng total saponins by ultra-performance liquid chromatography coupled with hybrid triple quadrupole-linear ion trap mass spectrometry. *RSC Adv.* 2016; *6*: 96376–96388.

Chen J, Tan M, Zou L, Liu X, Chen S, Shi J, Chen C, Wang C, Mei Y. Qualitative and Quantitative Analysis of the Saponins in Panacis Japonici Rhizoma using ultra-fast liquid chromatography coupled with triple quadrupole-time of flight tandem mass spectrometry and ultra-fast liquid chromatography coupled with triple quadrupole-linear ion trap tandem mass spectrometry. *Chem. Pharm. Bull.* 2019; *67*: 839–848.

Chen S, Wu BH, Fang JB, Liu YL, Zhang HH, Fang LC, Guan L, Li SH. Analysis of flavonoids from lotus (*Nelumbo nucifera*) leaves using high performance liquid chromatography/photodiode array detector tandem electrospray ionization mass spectrometry and an extraction method optimized by orthogonal design. *J. Chromatogr. A.* 2012; *1227*: 145–153.

Claeys M, Van den Heuvel H, Chen S, Derrick PJ, Mellon F, Price KR. Comparison of high- and low energy collision-induced dissociation tandem mass spectrometry in the analysis of glycoalkaloids and their aglycons. *J. Am. Soc. Mass Spectrom.* 1996; *7*: 173–181.

Colson E, Decroo C, Cooper-Shepherd D, Caulier G, Henoumont C, Laurent S, De Winter J, Flammang P, Palmer M, Claereboudt J, Gerbaux P. Discrimination of regioisomeric and stereoisomeric saponins from *Aesculus hippocastanum* seeds by ion mobility mass spectrometry. *J. Am. Soc. Mass Spectrom.* 2019; *30*: 2228–2237.

Colson E, Savarino P, Claereboudt E, Cabrera-Barjas G, Deleu M, Lins L, Eeckhaut I, Flammang P, Gerbaux P. Enhancing the membranolytic activity of *Chenopodium quinoa* saponins by fast microwave hydrolysis. *Molecules.* 2020; *25*: 1731.

Costello CE. 1996. Application of tandem mass spectral approaches to structural determinations of saponins. In: Waller GR, Yamasaki K, editors. *Saponins used in food and agriculture*. Boston: Springer. p 317–330.

Dai YL, Kim EA, Luo HM, Jiang YF, Oh JY, Heo SJ, Jeon YJ. Characterization and anti-tumor activity of saponin-rich fractions of South Korean sea cucumbers (*Apostichopus japonicus*). *J. Food Sci. Technol.* 2020; 57: 2283–2292.

Decroo C, Colson E, Demeyer M, Lemaur V, Caulier G, Eeckhaut I, Cornil J, Flammang P, Gerbaux P. Tackling saponin diversity in marine animals by mass spectrometry: data acquisition and integration. *Anal. Bioanal. Chem.* 2017; 409: 3115–3126.

Decroo C, Colson E, Lemaur V, Caulier G, De Winter J, Cabrera-Barjas G, Cornil J, Flammang P, Gerbaux P. Ion mobility mass spectrometry of saponin ions. *Rapid Commun. Mass Spectrom.* 2019; 33: 22–33.

Demeyer M, De Winter J, Caulier G, Eeckhaut I, Flammang P, Gerbaux P. Molecular diversity and body distribution of saponins in the sea star Asterias rubens by mass spectrometry. *Comp. Biochem. Physiol. Part B Biochem. Mol. Biol.* 2014; 168: 1–11.

Demeyer M, Wisztorski M, Decroo C, De Winter J, Caulier G, Hennebert E, Eeckhaut I, Fournier I, Flammang P, Gerbaux P. Inter- and intra-organ spatial distributions of sea star saponins by MALDI imaging. *Anal. Bioanal. Chem.* 2015; 407: 8813–8824.

Desai SD, Desai DG, Kaur H. Saponins and their biological activities. *Pharma Times.* 2009; 41: 13–16.

Domon B, Costello CE. A systematic nomenclature for carbohydrate fragmentations in FAB-MS/MS spectra of glycoconjugates. *Glycoconj. J.* 1988; 5: 397–409.

Gabelica V, Marklund E. Fundamentals of ion mobility spectrometry. *Curr. Opin. Chem. Biol.* 2018; 42: 51–59.

Gadea A, Fanuel M, Le Lamer AC, Boustie J, Rogniaux H, Charrier M, Lohézic-Le Devehat F. Mass spectrometry imaging of specialized metabolites for predicting lichen fitness and snail foraging. *Plants.* 2020; 9: 70.

Garneau FX, Simard JL, Harvey O, Apsimon JW, Girard M. The structure of psoluthurin A, the major triterpene glycoside of the sea cucumber Psolus fabricii. *Can. J. Chem.* 1983; 61: 1465–1471.

Gevrenova R, Bardarov V, Bardarov K, Voutquenne-Nazabadioko L, Henry M. Selective profiling of saponins from *Gypsophila trichotoma* Wend. by HILIC separation and HRMS detection. *Phytochem. Anal.* 2018; 29: 250–274.

Gevrenova R, Doytchinova I, Kołodziej B, Henry M. In-depth characterization of the GOTCAB saponins in seven cultivated *Gypsophila* L. species (Caryophyllaceae) by liquid chromatography coupled with quadrupole-Orbitrap mass spectrometer. *Biochem. Syst. Ecol.* 2019; 83: 91–102.

Ghisalberti EL. Steroidal glycoalkaloids: IsolatiOn, Structure, Analysis, And Biosynthesis. *Nat. Prod. Commun.* 2006; 1: 859–884.

Giles K, Ujma J, Wildgoose J, Pringle S, Richardson K, Langridge D, Green M. A cyclic ion mobility-mass spectrometry system. *Anal. Chem.* 2019; 91: 8564–8573.

Ha YW, Na YC, Seo JJ, Kim SN, Linhardt RJ, Kim YS. Qualitative and quantitative determination of ten major saponins in Platycodi Radix by high performance liquid chromatography with evaporative light scattering detection and mass spectrometry. *J. Chromatogr. A.* 2006; 1135: 27–35.

Habicht SD, Kind V, Rudloff S, Borsch C, Mueller AS, Pallauf J, Yang R, Krawinkel MB. Quantification of antidiabetic extracts

and compounds in bitter gourd varieties. *Food Chem.* 2011; 126: 172–176.

Haralampidis K, Trojanowska M, Osbourn AE. Biosynthesis of triterpenoid saponins in plants. *Adv. Biochem. Eng. Biotechnol.* 2002; 75: 31–49.

Havlíková L, Macáková K, Opletal L, Solich P. Rapid determination of α-hederin and hederacoside C in extracts of *Hedera helix* leaves available in the Czech Republic and Poland. *Nat. Prod. Commun.* 2015; 10: 1529–1531.

He Y, Liu W, Su R, Xiu Y, Pei J. Detection of saponins and oligosaccharides in herbs using direct analysis in real-time mass spectrometry. *Chem. Res. Chinese Univ.* 2017; 33: 172–178.

Huang FQ, Dong X, Yin X, Fan Y, Fan Y, Mao C, Zhou W. A mass spectrometry database for identification of saponins in plants. *J. Chrom. A.* 2020; 1625: 461296.

Ikekawa N, Natori S, Itokawa H, Tobinaga S, Matsui M. Gas chromatography of triterpenes. I. Ursanane, oleanane, and lupane groups. *Chem. Pharm. Bull.* 1965; 13: 316–319.

Jeong EK, Ha IJ, Kim YS, Na YC. Glycosylated platycosides: Identification by enzymatic hydrolysis and structural determination by LC-MS/MS. *J. Sep. Sci.* 2014; 37: 61–68.

Jæger D, Ndi CP, Crocoll C, Simpson BS, Khakimov B, Guzman-Genuino RM, Hayball JD, Xing X, Bulone V, Weinstein P, Møller BL, Semple SJ. Isolation and structural characterization of echinocystic acid triterpenoid saponins from the australian medicinal and food plant *Acacia ligulata*. *J. Nat. Prod.* 2017; 80: 2692–2698.

Kafle B, Baak J, Brede C. Quantification by LC–MS/MS of astragaloside IV and isoflavones in Astragali radix can be more accurate by using standard addition. *Phytochem. Anal.* 2020; 32: 466–473.

Kalinin VI, Prokofieva NG, Likhatskaya GN, Schentsova EB, Agafonova IG, Avilov SA, Drozdova OA. Hemolytic activities of triterpene glycosides from the holothurian order dendrochirotida: Some trends in the evolution of this group of toxins. *Toxicon.* 1996; 34: 475–483.

Kanchanapoom T, Kasai R, Yamasaki K. Acetylated triterpene saponins from the Thai medicinal plant, *Sapindus emarginatus*. *Chem. Pharm. Bull.* 2001; 49: 1195–1197.

Kang HK, Seo C, Park Y. The effects of marine carbohydrates and glycosylated compounds on human health. *Int. J. Mol. Sci.* 2015; 16: 6018–6056.

Kassem AS, Ahmed AM, Tariq MR. Study of saponins in methanol extract of the leaves of Acacia etbaica subspecies etbaica. *Res. J. Pharm. Biol. Chem. Sci.* 2014; 5: 803–810.

Khorlin AY, Chirva VY, Kochetkov NK. Triterpenoid saponins communication 15. Clematoside C-A triterpenoid olioside from the roots of the manchurian clematis (*Clematis manshurica* RUPR.). *Bull. Acad. Sci. USSR Div. Chem. Sci.* 1965; 14: 790–795.

Kim HJ, Park SR, Jang YP. Extraction-free in situ derivatisation of timosaponin aiii using direct analysis in real time TOF/MS. *Phytochem. Anal.* 2014; 25: 373–377.

Kite GC, Howes MJR, Simmonds MSJ. Metabolomic analysis of saponins in crude extracts of Quillaja saponaria by liquid chromatography/mass spectrometry for product authentication. *Rapid Commun. Mass Spectrom.* 2004; 18: 2859–2870.

Kofler L, Adam PA. Die Wertbestimmung der Saponindrogen. *Arch. Pharm. (Weinheim).* 1927; 265: 624–652.

Kuljanabhagavad T, Thongphasuk P, Chamulitrat W, Wink M. Triterpene saponins from *Chenopodium quinoa* Willd. *Phytochemistry.* 2008; 69: 1919–1926.

Le AV, Parks SE, Nguyen MH, Roach PD. Improving the vanillin-sulphuric acid method for quantifying total saponins. *Technologies* 2018; 6: 84.

Li B, Bhandari DR, Janfelt C, Römpp A, Spengler B. 2014. Natural products in *Glycyrrhiza glabra* (licorice) rhizome imaged at the cellular level by atmospheric pressure matrix-assisted laser desorption/ionization tandem mass spectrometry imaging. *Plant J.* 80:161–171.

Li W, Sun Y, Wang Z, Zheng Y. Isolation and purification of saponins from Platycodon grandiflorum by semi-preparative high performance liquid chromatography and LC-ESI/MS. *J. Liq. Chromatogr. Relat. Technol.* 2012; 35: 547–557.

Lin S, Wang D, Yang D, Yao J, Tong Y, Chen J. Characterization of steroidal saponins in crude extract from *Dioscorea nipponica* Makino by liquid chromatography tandem multi-stage mass spectrometry. *Anal. Chim. Acta.* 2007; 599: 98–106.

Liu G, Zhang Z, Lv X, Zhan S, Ding B, Yang X, Zhu Q. Localization of malonyl and acetyl on substituted saikosaponins according to the full-scan mass spectra and the fragmentation of sodium-adduct ions in the positive mode. *Rapid Commun. Mass Spectrom.* 2019; 33: 883–893.

Liu XH, Zhu RJ, Hu F, Guo L, Yang YL, feng SI. Tissue distribution of six major bio-active components after oral administration of Zhenqi Fuzheng capsules to rats using ultra-pressure liquid chromatography-tandem mass spectrometry. *J.Chrom.B.* 2015; 986-987: 44–53.

Liu Y, Su B, Wang X. Study on the noncovalent interactions of saikosaponins and cytochrome c by electrospray ionization mass spectrometry. *Rapid Commun. Mass Spectrom.* 2012; 26: 719–727.

Mackie AM, Grant PT, Lasker R. Avoidance reactions of a mollusc Buccinum undatum to saponin-like surface-active substances in extracts of the starfish Asterias rubens and Marthasterias glacialis. *Comp. Biochem. Physiol.* 1968; 26: 415–428.

Mackie AM, Singh HT, Fletcher TC. Studies on the cytolytic effects of seastar (Marthasterias glacialis) saponins and synthetic surfactants in the plaice Pleuronectes platessa. *Mar. Biol.* 1975; 29: 307–314.

Maier MS. 2008. Biological activities of sulfated glycosides from echinoderms. In: Rahman AU, editor. *Studies in natural products chemistry.* Amsterdam: Elsevier B.V. p 311–354.

McKey D. Adaptive patterns in alkaloid physiology. *Am. Nat.* 1974; 108: 305–320.

Mert-Türk F, Osbourn A. Saponins versus plant fungal pathogens. *Trends Plant Sci.* 2006; 5: 13–17.

Mesleh MF, Hunter JM, Shvartsburg AA, Schatz GC, Jarrold MF. Structural information from ion mobility measurements: Effects of the long-range potential. *J. Phys. Chem.* 1996; 100: 16082–16086.

Moghimipour E, Handali S. Saponin: properties, methods of evaluation and applications. *Annu. Res. Rev. Biol.* 2015; 5: 207–220.

Nord LI, Kenne L. Separation and structural analysis of saponins in a bark extract of *Quillaja saponaria* Molina. *Carbohydr. Res.* 1999; 320: 70- 81.

Nyakudya E, Jeong JH, Lee NK, Jeong YS. Platycosides from the roots of platycodon grandiflorum and their health benefits. *Prev. Nutr. Food Sci.* 2014; 19: 59–68.

Oleszek W, Hamed A. 2010. Saponin-based surfactants. In: Kjellin M, Johansson I, editors. *Surfactants from renewable resources.* New Jersey: John Wiley & Sons. p 239–249.

Osbourn AE, Qi X, Townsend B, Qin B. Dissecting plant secondary metabolism—Constitutive chemical defences in cereals. *New Phytol.* 2003; 159: 101–108.

Pettolino FA, Walsh C, Fincher GB, Bacic A. Determining the polysaccharide composition of plant cell walls. *Nat. Protoc.* 2012; 7: 1590–1607.

Le Pogam P, Legouin B, Geairon A, Rogniaux H, Lohézic-Le Dévéhat F, Obermayer W, Boustie J, Le Lamer AC. Spatial mapping of lichen specialized metabolites using LDI-MSI: Chemical ecology issues for Ophioparma ventosa. *Sci. Rep.* 2016; 6: 37807.

Popov RS, Ivanchina NV, Silchenko AS, Avilov SA, Kalinin VI, Dolmatov IY, Stonik VA, Dmitrenok PS. Metabolite profiling of triterpene glycosides of the far eastern sea cucumber Eupentacta fraudatrix and their distribution in various body components using LC-ESI QTOF-MS. *Mar. Drugs.* 2017; 15: 302.

Prome J-C, Aurelle H, Prome D, Savagnac A. Gas phase glycosidic cleavage of oxynions from alkyl glycosides. *Org. Mass Spectrom.* 1987; 22: 6–12.

Qu C, Yang L, Yu S, Wang S, Bai Y, Zhang H. Investigation of the interactions between ginsenosides and amino acids by mass spectrometry and theoretical chemistry. *Spectrochim. Acta Part A Mol. Biomol. Spectrosc.* 2009; 74: 478–483.

Quinn R, Basanta-Sanchez M, Rose RE, Fabris D. Direct infusion analysis of nucleotide mixtures of very similar or identical elemental composition. *J. Mass Spectrom.* 2013; 48: 703–712.

Rodriguez J, Castro R, Riguera R. Holothurinosides: New antitumour non sulphated triterpenoid glycosides from the sea cucumber Holothuria forskalii. *Tetrahedron.* 1991; 47: 4753–4762.

Sahu NP, Banerjee S, Mondal NB, Mandal D. Steroidal saponins. *Fortschr. Chem. Org. Naturst.* 2008; 89: 45–141.

Sandvoss M, Pham LH, Levsen K, Preiss A, Mügge C, Wünsch G. Isolation and structural elucidation of steroid oligoglycosides from the starfish Asteria rubens by means of direct online LC-NMR-MS hyphenation and one- and two-dimensional NMR investigations. *Eur. J. Org. Chem.* 2000; 2000: 1253–1262.

Sandvoss M, Preiss A, Levsen K, Weisemann R, Spraul M. Two new asterosaponins from the starfish Asteria rubens: Application of a cryogenic NMR probe head. *Magn. Reson. Chem.* 2003; 41: 949–954.

Sandvoss M, Weltring A, Preiss A, Levsen K, Wuensch G. Combination of matrix solid-phase dispersion extraction and direct on-line liquid chromatography–nuclear magnetic resonance spectroscopy–tandem mass spectrometry as a new efficient approach for the rapid screening of natural products: *J. Chromatogr. A.* 2001; 917: 75–86.

Shi J, Cai Z, Chen S, Zou L, Liu X, Tang R, Ma J, Wang C, Chen J, Tan M. Qualitative and quantitative analysis of saponins in the flower bud of *Panax ginseng* (Ginseng Flos) by UFLC-Triple TOF-MS/MS and UFLC-QTRAP-MS/MS. *Phytochem. Anal.* 2020; 31: 287–296.

Shvartsburg AA, Jarrold MF. An exact hard-spheres scattering model for the mobilities of polyatomic ions. *Chem. Phys. Lett.* 1996; 261: 86–91.

De Simone F, Dini A, Finamore E, Minale L, Pizza C, Riccio R, Zollo F. Starfish saponins. Part 5. Structure of sepositoside A, a

novel steroidal cyclic glycoside from the starfish *Echinaster sepositus*. *J. Chem. Soc. Perkin Trans*. 1981; 1: 1855–1862.

Song F, Cui M, Liu Z, Yu B, Liu S. Multiple-stage tandem mass spectrometry for differentiation of isomeric saponins. *Rapid Commun. Mass Spectrom*. 2004; 18: 2241–2248.

Song F, Liu Z, Liu S, Cai Z. Differentiation and identification of ginsenoside isomers by electrospray ionization tandem mass spectrometry. *Anal. Chim. Acta*. 2005; 531: 69–77.

Stonik VA. Some terpenoid and steroid derivatives from echinoderms and sponges. *Pure Appl. Chem*. 1986; 58: 423–436.

Taira S, Ikeda R, Yokota N, Osaka I, Sakamoto M, Kato M, Sahashi Y. Mass Spectrometric imaging of ginsenosides localization in *Panax ginseng* Root. *Am. J. Chin. Med*. 2010; 38: 485–493.

Uetrecht C, Rose RJ, van Duijn E, Lorenzen K, Heck AJR. Ion mobility mass spectrometry of proteins and proteinassemblies. *Chem. Soc. Rev*. 2010; 39: 1633–1655.

Van Dyck S, Caulier G, Todesco M, Gerbaux P, Fournier I, Wisztorski M, Flammang P. The triterpene glycosides of *Holothuria forskali*: Usefulness and efficiency as a chemical defense mechanism against predatory fish. *J. Exp. Biol*. 2011; 214: 1347–1356.

Van Dyck S, Flammang P, Meriaux C, Bonnel D, Salzet M, Fournier I, Wisztorski M. Localization of secondary metabolites in marine invertebrates: Contribution of MALDI MSI for the study of saponins in cuvierian tubules of *H. forskali*. *PLOS One*. 2010; 5: e13923.

Van Dyck S, Gerbaux P, Flammang P. Elucidation of molecular diversity and body distribution of saponins in the sea cucumber Holothuria forskali (Echinodermata) by mass spectrometry. Comp. Biochem. Physiol. Part B Biochem. *Mol. Biol*. 2009; 152: 124–134.

Van Dyck S, Gerbaux P, Flammang P. Qualitative and quantitative saponin contents in five sea cucumbers from the Indian ocean. *Mar. Drugs*. 2010; 8: 173–189.

Vincken JP, Heng L, de Groot A, Gruppen H. Saponins, classification and occurrence in the plant kingdom. *Phytochemistry*. 2007; 68: 275–297.

Wang W, Wang GJ, Xie HT, Sun JG, Zhao S, Jiang XL, Li H, Xu HLMJ, Wang R. Determination of ginsenoside Rd in dog plasma by liquid chromatography–mass spectrometry after solid-phase extraction and its application in dog pharmacokinetics studies. *J. Chromatogr. B*. 2007; 852: 8–14.

Wang W, Zhao Y, Jing W, Zhang J, Xiao H, Zha Q, Liu A. Ultrahigh-performance liquid chromatography-ion trap mass spectrometry characterization of the steroidal saponins of *Dioscorea panthaica* Prain et Burkill and its application for accelerating the isolation and structural elucidation of steroidal saponins. *Steroids*. 2015; 95: 51–65.

Wei F, Ma LY, Cheng XL, Lin RC, Jin WT, Khan IA, Lu JQ. Preparative HPLC for purification of four isomeric bioactive saponins from the seeds of Aesculus chinensis. *J. Liq. Chromatogr. Relat. Technol*. 2005; 28: 763–773.

Wu X, Jia L, Wu J, Liu Y, Kang H, Liu X, Li P, He P, Tu Y, Li B. Simultaneous Determination and quantification of triterpene saponins from *Camellia sinensis* seeds using UPLC-PDA-QTOF-MS/MS. *Molecules*. 2019; 24: 3794.

Xu H, Ji X, Shi X, Du Y, Zhu H, Zhang L. Development of a novel method for triterpenoidal saponins in rat plasma by solid-phase extraction and high-performance liquid chromatography tandem mass spectrometry. *Anal. Biochem*. 2011; 419: 323–332.

Xu HJ, Shi XW, Ji X, Du YF, Zhu H, Zhang LT. A rapid method for simultaneous determination of triterpenoid saponins in *Pulsatilla turczaninovii* using microwave-assisted extraction and high performance liquid chromatography–tandem mass spectrometry. *Food Chemistry*. 2012; 135: 251–258.

Yang Y, Laval S, Yu B. Chemical synthesis of saponins. *Adv. Carbohydr. Chem. Biochem*. 2014; 71: 137–226.

Yang Y, Yang Y, Qiu H, Ju Z, Shi Y, Wang Z, Yang L. Localization of constituents for determining the age and parts of ginseng through ultraperfomance liquid chromatography quadrupole/time of flight-mass spectrometry combined with desorption electrospray ionization mass spectrometry imaging. *J. Pharm. Biomed. Anal*. 2021; 193: 113722.

Yasumoto T, Tanaka M, Hashimo Y. Distribution of saponin in echinoderms. *Nippon Suisan Gakkaishi*. 1966; 32: 673–676.

Yoshikawa M, Murakami T, Matsuda H, Yamahara J, Murakami N, Kitagawa I. Bioactive saponins and glycosides. III. Horse chestnut. (1): The structures, inhibitory effects on ethanol absorption, and hypoglycemic activity of escins Ia, Ib, IIa, IIb, and IIIa from the seeds of *Aesculus hippocastanum* L. *Chem. Pharm. Bull*. 1996; 44: 1454–1464.

Zehl M, Pittenauer E, Jirovertz L, Bandhari P, Singh B, kaul VK, Rizzi A, Allmaier G. Multistage and tandem mass spectrometry of glycosylated triterpenoid saponins isolated from *Bacopa monnieri*: Comparison of the information content provided by different techniques. *Anal. Chem*. 2007; 79: 8214–8221.

Zhang H, Ding L, Qu C, Li D, Zhang H. Study on the noncovalent complexes of ginsenoside and cytochrome c by electrospray ionization mass spectrometry. *Spectrochim. Acta Part A Mol. Biomol. Spectrosc*. 2007; 68: 312–316.

Zhang PC, Zheng CF, Wu CS, Sheng YX, Zhang JL. Mass spectral fragmentation analysis of triterpene saponins from Ardisia crenata Sims by electrospray ionization Fourier transform ion cyclotron resonance mass spectrometry. *J. Asian Nat. Prod. Res*. 2010; 12: 64–69.

Zhang X, Li J, Ito Y, Sun W. Simultaneous quantification of five steroid saponins from *Dioscorea zingiberensis* C.H. Wright in rat plasma by HPLC–MS/MS and its application to the pharmacokinetic studies. *Steroids*. 2015; 93: 16–24.

Zheng W, Wang F, Zhao Y, Sun X, Kang L, Fan Z, Qiao L, Yan R, Liu S, Ma B. Rapid characterization of constituents in tribulus terrestris from different habitats by UHPLC/Q-TOF MS. *J. Am. Soc. Mass Spectrom*. 2017; 28: 2302–2318.

AUTHOR BIOGRAPHIES

Philippe Savarino obtained his MSc degree in Chemistry from the University of Mons, Belgium, in 2019. He is currently PhD student in the Laboratory of Organic Synthesis and Mass Spectrometry (S²MOs) at the University of Mons and the Laboratory of Phytopathology, Microbial and Molecular Farming (PMMF) at the "Haute Ecole Provinciale du Hainaut Condorcet", under the supervision of Prof Pascal

Gerbaux and Dr Nicolas Desoignies. His work focuses on the evaluation of saponins as bio-based fungicides for organic farming via a structure/activity approach by mass spectrometry.

Marie Demeyer obtained her PhD in Chemistry from the University of Mons, Belgium, in 2015. Her thesis focused on the study of the saponins of the starfish *Asterias rubens* by mass spectrometry under the supervision of Prof Pascal Gerbaux (Laboratory of Organic Synthesis and Mass Spectrometry - S^{2}MOs) and Prof Patrick Flammang (Biology of Marine Organisms and Biomimetism – BOMB). She is currently Project Associate at Certech (Seneffe) in the materials and environment group. Her work consists in evaluating the VOC (volatil organic compounds) emissions emitted by automotive interior materials by GC-MS analyses.

Decroo Corentin obtained his PhD in Sciences from the University of Mons – Belgium – in 2018. The thesis subject consisted in the application of ion mobility mass spectrometry to achieve the full structural characterization of saponins extracted from plants and marine animals. This thesis was conducted under the supervision of Prof Pascal Gerbaux (Laboratory of Organic Synthesis and Mass Spectrometry - S^{2}MOs) and Prof Patrick Flammang (Biology of Marine Organisms and Biomimetism – BOMB) in collaboration with Dr. Jérôme Cornil (Laboratory for Chemistry of Novel Materials – CMN). He is currently Scientific Coordinator in the Bioprofiling platform (UMONS-ULB) - part of MS QUANTA (UMONS-ULIEGE). His work consists in MRM method development for biomarkers (Peptides/Proteins) found in bacteria, tissues, or cells.

Emmanuel Colson graduated from the University of MONS (UMONS), Belgium in 2020. He realized his PhD thesis within the Laboratory of Organic Synthesis and Mass Spectrometry (S^{2}MOs), in partnership with the Biology of Marine Organisms and Biomimetics laboratory (BOMB) at UMONS under the supervision of Prof Pascal Gerbaux and Prof Patrick Flammang. His thesis focused on green waste valorization by tuning the biological properties of horse chestnut and quinoa husk saponins. He actually works as scientist at Quality Assistance (Thuin), a company offering product-dedicated expertise in analytical sciences.

Pascal Gerbaux has obtained his PhD in Science from the University of Mons-Hainaut in 1999 under the supervision of Prof Robert Flammang. After having completed several postdoctoral stays abroad, i.e. Ecole Polytechnique de Palaiseau, University of Washington and University of Utrecht, he got a permanent position at the University of Mons as a F.N.R.S. Senior Research Associate. For years, his research topics are related to the study of gas phase ions using mass spectrometry methods. He is now Full Professor of organic chemistry and mass spectrometry and head of the Organic Synthesis and Mass Spectrometry Laboratory at UMONS.